



Communications  
Research Centre  
Centre de recherches  
sur les communications

# Field Trial Evaluation of the CRC Adaptive-Antenna Algorithm for the NATO STANAG 4285 Waveform

*by*

K.H. Wu and A. Tenne-Sens

CRC REPORT NO. 97-004

December 1997  
Ottawa

TK  
5102.5  
C673e  
#97-004



Industry  
Canada

Industrie  
Canada

IC

The work was sponsored by the Department of National Defence,  
Research and Development Branch, under Project No. 998426156.

Canada

TK  
5102.5  
C673e  
#97-004  
e.b  
S-Gen

## ABSTRACT

Results are presented for the evaluation of an adaptive antenna algorithm designed for the NATO STANAG 4285 (FSII) (phase shift keying) waveform. The algorithm was developed at the Communications Research Centre (CRC) and has been implemented on both the Analog-to-Digital (A/D) Adaptive Antenna Receiver System (AARS) and the Digital-to-Analog (D/A) Adaptive Antenna Receiver System (AARS). The test system was used to evaluate the algorithm's performance in a line-of-sight environment.

# Field Trial Evaluation of the CRC Adaptive-Antenna Algorithm for the NATO STANAG 4285 Waveform

by

**K.H. Wu and A. Tenne-Sens**

*Advanced Radio Systems Group*

*Radio Communications Technologies Directorate*

CRC LIBRARY  
-03- 30 1998  
BIBLIOTHEQUE

Industry Canada  
Library - Queen

AUG 22 2012

Industrie Canada  
Bibliothèque - Queen

The work was sponsored by the Department of National Defence, Research and Development Branch, under Project No. 998426156.

**INDUSTRY CANADA**  
CRC REPORT NO. 97-004

Canada

December 1997  
Ottawa



## ABSTRACT

Results are presented for the evaluation of an adaptive-antenna algorithm designed for the NATO STANAG 4285 PSK (phase-shift keyed) waveform. The algorithm was developed at the Communications Research Centre (CRC) and has been implemented on both the Andrew SciComm HF Adaptive-Antenna Receiving System (HFAARS or AN/FRQ-26) and the SED Systems Programmable HF Adaptive Receiving System (PHFARS); the tests reported here were conducted using the Andrew HFAARS. The goal was to evaluate the antijamming capability for groundwave or line-of-sight communications in the presence of various types of jamming signals. Performance of the system was characterized in terms of bit-error rate (BER) versus jamming-to-signal ratio (J/S) under various signal, jamming, and propagation conditions. Under most of the test conditions reported, the algorithm was able to suppress the jamming signals by at least 40 dB.

## RÉSUMÉ

Ce rapport décrit les résultats de l'évaluation d'un algorithme d'antennes adaptatives, développé pour une modulation par déplacement de phase tel que décrit dans le standard STANAG 4285 de l'OTAN. Cet algorithme a été développé au Centre de recherches sur les communications (CRC) et a été implémenté sur le système HFAARS ("HF Adaptive Antenna Receiving System") aussi appelé AN/FRQ-26 de la société Andrew SciComm, ainsi que sur le système PHFARS ("Programmable HF Adaptive Receiving System") de la société SED Systems. Les évaluations décrites dans ce rapport ont été conduites sur le système HFAARS. Le but de ces évaluations était de mesurer l'efficacité antibrouillage de l'algorithme pour des communications par propagation directe ou par le sol en présence de divers types de signaux de brouillage. La performance du système est décrite par le taux d'erreur (BER) en fonction du rapport brouillage-signal (J/S) pour divers types de signaux, types de brouillage, et conditions de propagation d'ondes. Pour la plupart des conditions d'évaluation considérées dans cette étude, l'algorithme fut capable de réduire le niveau du signal de brouillage par au moins 40 dB.





## EXECUTIVE SUMMARY

A field-trial evaluation of an adaptive-antenna algorithm was conducted using local over-the-air signals. The algorithm was developed at CRC for the NATO STANAG 4285 PSK (phase-shift keyed) waveform, and was run on the Andrew HFAARS<sup>1</sup> (AN/FRQ-26) and the SED Systems PHFARS<sup>2</sup>. The goal was to evaluate the antijamming capability over land in the presence of various types of jamming signals: continuous-noise, pulsed-noise, and chirp jamming. The HFAARS was installed in the laboratory at CRC with four receiving antennas mounted on the roof the building. Some of the preliminary tests were conducted using a cable network instead of the antennas, which simulates an ideal propagation environment. Performance of the system was characterized in terms of the bit-error rate (BER) versus jamming-to-signal ratio (J/S) under various signal, jamming, and propagation conditions.

For a single jammer of any of the tested types the experiments showed that:

1. Very low values of BER were obtained, in most cases for J/S up to 30 dB.
2. When the error-correcting mode of the 4285 waveform was used, low post-correction values of BER were obtained for J/S up to at least 45 dB — a power ratio of over 30 000.

The large reduction of J/S achieved by the algorithm can therefore render brute-force jamming ineffective.

These tests show that the algorithm is suitable for incorporation into commercial antijamming HF radio systems for military applications. Also, the digital signal processing (DSP) techniques described herein do not depend on the signal's carrier frequency. Similar techniques can therefore be used at higher frequencies, such as the current mobile communications frequencies in the VHF and UHF bands.

---

<sup>1</sup> HFAARS stands for High Frequency Adaptive-Antenna Receiving System. The system was designed and manufactured by Andrew Corporation in Australia. The proprietary rights of the HFAARS were transferred to Andrew SciComm in Garland, Texas after the Australian subsidiary was closed in 1992.

<sup>2</sup> PHFARS stands for Programmable High Frequency Adaptive Receiving System. An advanced development model (ADM) was designed by the first author at CRC and built by SED Systems Inc. in Saskatoon, Saskatchewan, Canada, under a contract sponsored by DND/DMSS 8. The ADM was completed in February 1997.



# TABLE OF CONTENTS

	Page
ABSTRACT / RÉSUMÉ	iii
EXECUTIVE SUMMARY	v
LIST OF FIGURES	ix
LIST OF TEST-RESULT CHARTS	xi
1.0 INTRODUCTION	1
2.0 THE 4285 WAVEFORM	1
3.0 OPERATIONAL DESCRIPTION OF THE 4285 WAVEFORM	3
4.0 TEST ARRANGEMENT	6
4.1 Laboratory Setup	7
4.2 Over-the-Air Setup	8
5.0 SIGNAL TRANSMISSIONS	11
5.1 Communications Transmissions	11
5.2 Jamming Transmissions	12
6.0 TEST PARAMETERS	14
7.0 DATA PRESENTATION	15
8.0 RESULTS	16
8.1 4-PSK Signals (Charts 1 – 13)	16
8.1.1 Continuous-Noise Jamming	16
8.1.2 Chirp Jamming	16
8.1.3 Pulsed-Noise Jamming	16
8.2 8-PSK Signals (Charts 14 – 21)	17
8.3 2-PSK Signals (Charts 22-24)	18
8.4 Performance Under Direct Control of Electrical Phase Angles of the Jamming Signals (Charts 25-32)	18
8.5 Multiple Jammers	19
9.0 CONCLUSIONS	20
ACKNOWLEDGEMENTS	20
REFERENCES	21
APPENDIX A: THE TEST MESSAGE	A-1
APPENDIX B: TEST RESULTS	B-1





## LIST OF FIGURES

	Page
Figure 1: Structure of the NATO STANAG 4285 waveform.	2
Figure 2: Simplified block diagram for the processing of the 4285 waveform.	4
Figure 3: Details of the processing algorithm for the 4285 waveform.	5
Figure 4: Performance curves for the error-correcting decoder implementation in the current version of the 4285 algorithm.	6
Figure 5: Diagram of the upconversion circuit for the desired signal and jammer.	7
Figure 6: Simulated signal scenario for the laboratory tests.	8
Figure 7: RF cable and splitter/combiner network to simulate the scenario of Figure 6.	9
Figure 8: Bird's-eye view of the antenna layout on top of the northwest end of CRC's Building 2 (not to scale).	9
Figure 9: Layout for the over-the-air measurements at the CRC site.	10
Figure 10: A sample of the pulsed-noise jamming waveform.	13
Figure 11: Frequency-sweep characteristic of the chirp jamming waveform.	13
Figure 12: Plot of maximum J/S for BER less than $10^{-3}$ , as a function of jammer phase increment.	19



## LIST OF TEST-RESULT CHARTS

	Page
Chart 1: 4-PSK, continuous-noise jamming, 28.738 MHz, laboratory test, uncoded.	B-1
Chart 2: 4-PSK, continuous-noise jamming, 3.53 MHz, over-the-air test, uncoded.	B-1
Chart 3: 4-PSK, continuous-noise jamming, 7.01 MHz, over-the-air test, uncoded.	B-2
Chart 4: 4-PSK, continuous-noise jamming, 10.1 MHz, over-the-air test, uncoded.	B-2
Chart 5: 4-PSK, chirp jamming, 10.1 MHz, over-the-air test, uncoded.	B-3
Chart 6: 4-PSK, chirp jamming, 7.01 MHz, over-the-air test, uncoded.	B-3
Chart 7: 4-PSK, pulsed-noise jamming, 10.1 MHz, over-the-air test, anti-pulse off, uncoded.	B-4
Chart 8: 4-PSK, pulsed-noise jamming, 10.1 MHz, over-the-air test, anti-pulse off, coded.	B-4
Chart 9: 4-PSK, pulsed-noise jamming, 28.738 MHz, laboratory test, uncoded.	B-5
Chart 10: 4-PSK, pulsed-noise jamming, 28.738 MHz, over-the-air test, uncoded.	B-5
Chart 11: 4-PSK, pulsed-noise jamming, 28.738 MHz, over-the-air test, coded.	B-6
Chart 12: 4-PSK, continuous-noise jamming, 28.738 MHz, over-the-air test, coded.	B-6
Chart 13: 4-PSK, chirp jamming, 28.738 MHz, over-the-air test, coded.	B-7
Chart 14: 8-PSK, continuous-noise jamming, 10.1 MHz, over-the-air test, uncoded.	B-7
Chart 15: 8-PSK, continuous-noise jamming, 28.738 MHz, over-the-air test, uncoded.	B-8
Chart 16: 8-PSK, chirp jamming, 10.1 MHz, over-the-air test, uncoded.	B-8
Chart 17: 8-PSK, chirp jamming, 28.738 MHz, over-the-air test, uncoded.	B-9
Chart 18: 8-PSK, pulsed-noise jamming, 28.738 MHz, over-the-air test, uncoded.	B-9
Chart 19: 8-PSK, continuous-noise jamming, 28.738 MHz, over-the-air test, coded.	B-10
Chart 20: 8-PSK, chirp jamming, 28.738 MHz, over-the-air test, coded.	B-10
Chart 21: 8-PSK, pulsed-noise jamming, 28.738 MHz, over-the-air test, coded.	B-11

	Page
Chart 22: 2-PSK, continuous-noise jamming, 3.573 MHz, over-the-air test, uncoded.	B-11
Chart 23: 2-PSK, chirp jamming, 3.573 MHz, over-the-air test, uncoded.	B-12
Chart 24: 2-PSK, pulsed-noise jamming, 3.573 MHz, over-the-air test, uncoded.	B-12
Chart 25: 4-PSK, continuous-noise jamming, 28.738 MHz, laboratory test, 0-degree jammer phase increments, uncoded.	B-13
Chart 26: 4-PSK, continuous-noise jamming, 28.738 MHz, laboratory test, 5-degree jammer phase increments, uncoded.	B-13
Chart 27: 4-PSK, continuous-noise jamming, 28.738 MHz, laboratory test, 10-degree jammer phase increments, uncoded.	B-14
Chart 28: 4-PSK, continuous-noise jamming, 28.738 MHz, laboratory test, 20-degree jammer phase increments, uncoded.	B-14
Chart 29: 4-PSK, continuous-noise jamming, 28.738 MHz, laboratory test, 45-degree jammer phase increments, uncoded.	B-15
Chart 30: 4-PSK, continuous-noise jamming, 28.738 MHz, laboratory test, 90-degree jammer phase increments, uncoded.	B-15
Chart 31: 4-PSK, continuous-noise jamming, 28.738 MHz, laboratory test, 135-degree jammer phase increments, uncoded.	B-16
Chart 32: 4-PSK, continuous-noise jamming, 28.738 MHz, laboratory test, 180-degree jammer phase increments, uncoded.	B-16



## 1.0 INTRODUCTION

This report presents a technical evaluation, conducted both in the laboratory and over the air, of the NATO STANAG 4285 Adaptive-Antenna Signal Processing Algorithm (known as "the 4285 algorithm" hereafter) developed at CRC. The software was designed to run on a modified version of the Andrew HFAARS intended for development purposes, and the SED Systems PHFARS intended as an operational prototype [1]. The results compiled in this report were gathered prior to completion of the PHFARS, using the Andrew HFAARS. The design of the 4285 algorithm and some preliminary performance evaluations are described in [2]. A sea trial that took place on the HMCS Saskatchewan destroyer escort warship in 1994 showed that the system was effective while using the ship's existing antennas [3]. A laboratory evaluation of the algorithm running in the SED Systems PHFARS is documented in a separate report [4].

The goal of the field trial was to conduct a thorough technical evaluation for the 4285 algorithm running on the HFAARS, both in the laboratory and over the air using local transmissions, before the sea trial took place. The performance of the HFAARS running the 4285 algorithm was characterized by the BER achieved. The major parameter of interest that governs BER is the ratio  $J/S$ . To ensure that antijamming performance is not limited by the system noise, the transmitting signal power was adjusted to provide a signal-to-noise power ratio ( $S/N$ ) of greater than 20 dB.

The present field trial was conducted on the CRC grounds. The HFAARS and the two transmitters, one for the desired signal and one for the jammer, were stationary. For over-the-air testing, the separation of the receiving antenna array from the transmitting antennas was less than one kilometer, hence propagation was either line-of-sight or via groundwave. Testing under a skywave-propagation environment is planned for the near future.

## 2.0 THE 4285 WAVEFORM

The NATO STANAG 4285 waveform is described in [5]. A brief description is given here to familiarize the reader with the different modes used in the technical evaluation.

The 4285 signal is a PSK-modulated serial waveform. There are three levels of phase shifting: 2-, 4- and 8-PSK.

The protocol for the 4285 waveform organizes the data stream into frames whose structure is shown in Figure 1. The structure is fixed and has slots, or blocks, that hold the message to be transmitted. The structure includes standard sequences intended for

synchronization and channel equalization, and which are used by the adaptive-antenna algorithm. These sequences are the same in all frames. Each frame starts with 80 predetermined symbols for synchronization. The synchronization symbols consist of a 31-bit m-sequence with 2-PSK coding, repeated two and a half times. The synchronization symbols are followed by four blocks reserved for the message. Each message block contains 32 symbols, and each symbol contains 1, 2, or 3 bits of information, depending on whether the symbols are 2-, 4-, or 8-PSK, respectively. Adjacent message blocks are separated by a reference block containing 16 zero-phase symbols. The message blocks and the reference blocks are scrambled by an 8-PSK fixed pseudorandom sequence. The synchronization block, which is already a pseudorandom sequence in itself, is not scrambled.

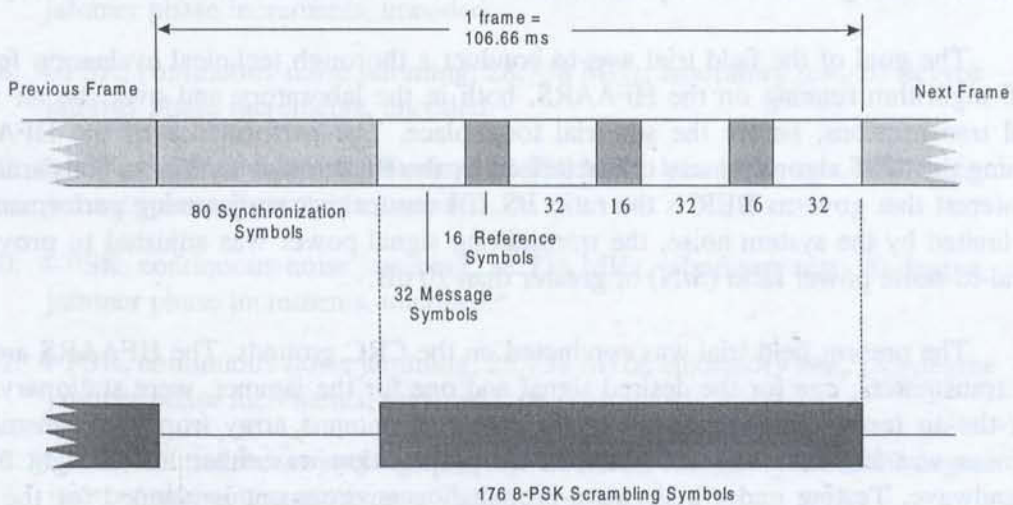


Figure 1: Structure of the NATO STANAG 4285 waveform.

The 4285 protocol includes an optional error-correction-coding scheme for the message data. Details of the encoding and decoding schemes are given in [5]. The coding scheme consists of an interleaver and a constraint-length 7, rate  $\frac{1}{2}$  convolutional encoder. The code is punctured to rate  $\frac{2}{3}$  to achieve 2400 bps when 8-PSK modulation is used.

Error-correction coding was not used in most of the present field trial cases because coding masks the real BER performance (i.e. the fraction of received bits that are different from those transmitted). Bit errors can be caused by propagation effects,

interference, or noise. The real BER is directly related to the effectiveness of the adaptive-antenna algorithm in cancelling interference or jamming. Error-correction coding can be considered as an add-on feature that further improves the BER after jamming suppression.

### **3.0 OPERATIONAL DESCRIPTION OF THE 4285 ALGORITHM**

STANAG 4285 is a general-purpose serial waveform for high data-rate HF transmission and was not specially designed for use with adaptive antennas. The reference blocks were originally intended for channel equalization by a single-receiver system. In the 4285 adaptive-antenna algorithm, the reference blocks are used for calculating the antenna weights. Details of this calculation are provided in [2]. The calculated weights are applied to the data contained in the message slots to cancel any potential jamming or interference signals.

A simplified block diagram for the processing procedure is shown in Figure 2. The adaptation functions following the HFAARS Data Preprocessor are all implemented in real-time software to run on the DSP chip used in the HFAARS, the Texas Instruments TMS320C40 (called the "C40" in this report) running at a clock speed of 40 MHz.

Once the 4285 algorithm is started, it actively searches for the onset of a 4285 signal regardless of whether or not jamming or other interfering signals are present. The synchronization symbols in the first frame are used for detecting the onset of the signal transmission. The detection portion of the algorithm takes advantage of the four correlated antenna outputs to recognize the synchronization symbols in the presence of strong jamming signals [2]. When a transmission is detected, synchronization follows immediately. The synchronization process fine-tunes the sampling timing so that the best match between the transmitted and received synchronization samples is obtained. If detection of the first frame fails, detection of subsequent frames is attempted automatically, and the message data contained in the missed frames are lost. After the detection and synchronization phase, subsequent frames are tracked and minor synchronization adjustment is performed on a frame-by-frame basis. At the end of the message, tracking is discontinued and the system returns to the search mode waiting for a new transmission to arrive.

Further details of the algorithm are given in Figure 3.

The 4285 algorithm also has a novel technique for suppressing pulsed jamming [2], further described in Section 5.2. The technique was tested by comparing the performance of two versions of the algorithm, one incorporating the technique ("anti-pulse on"), the other without it ("anti-pulse off").

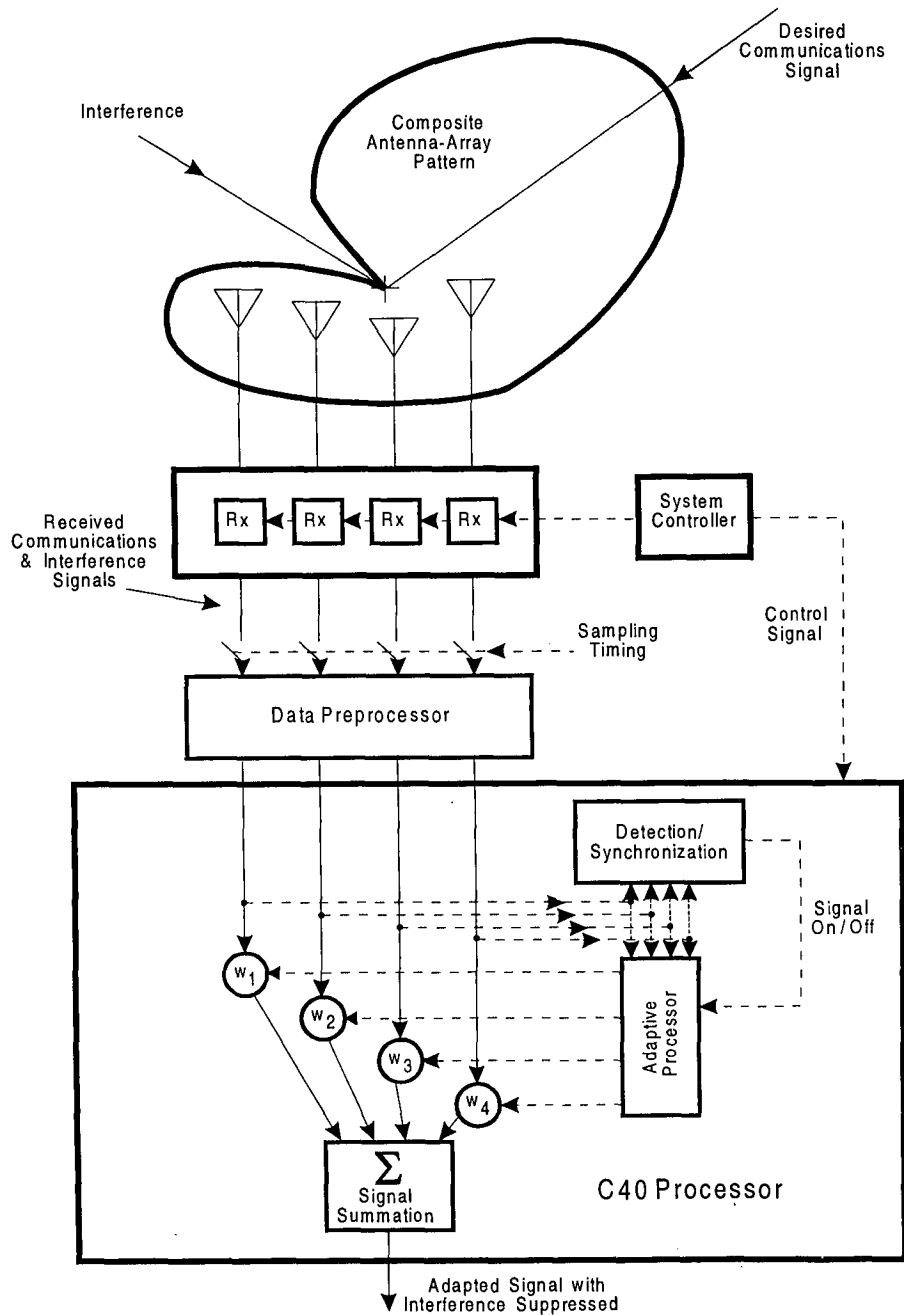


Figure 2: Simplified block diagram for the processing of the 4285 waveform.

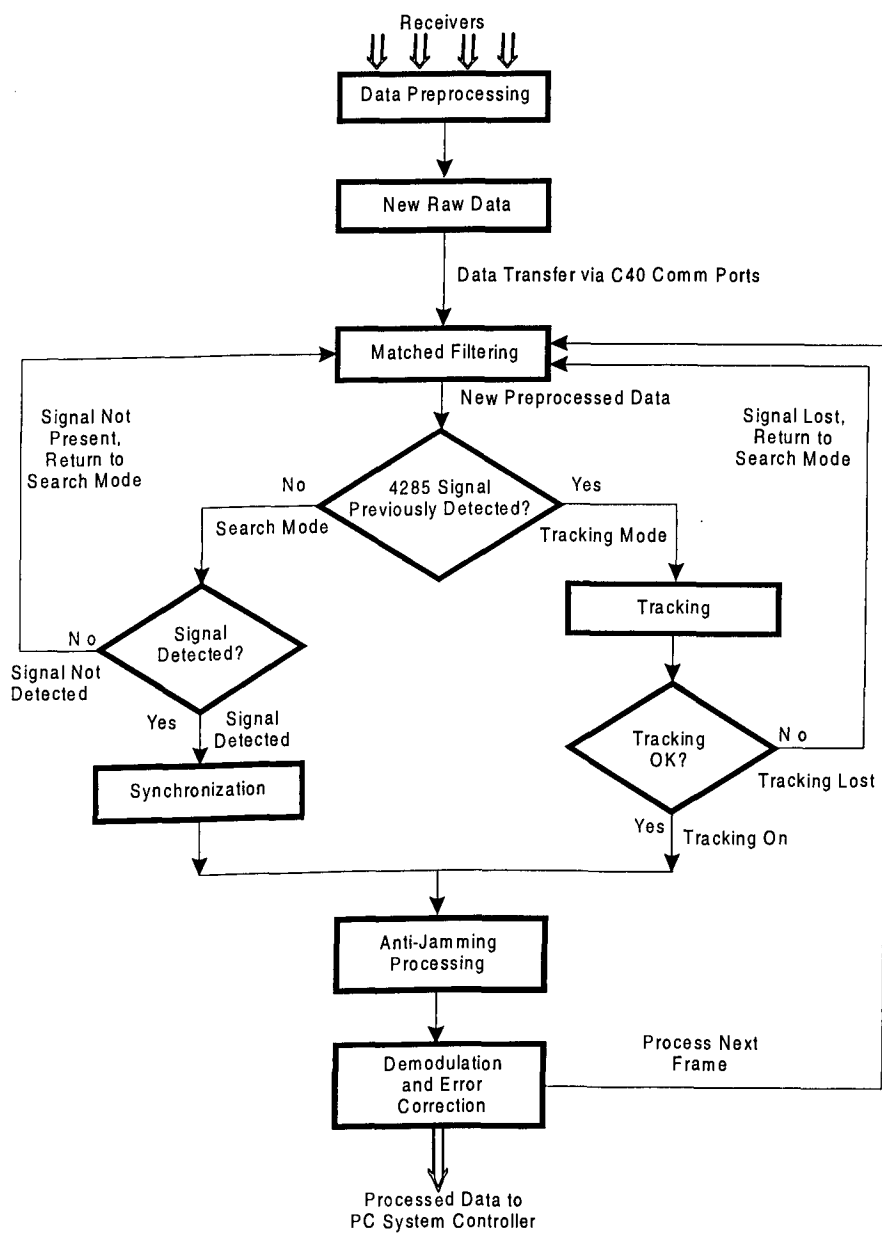
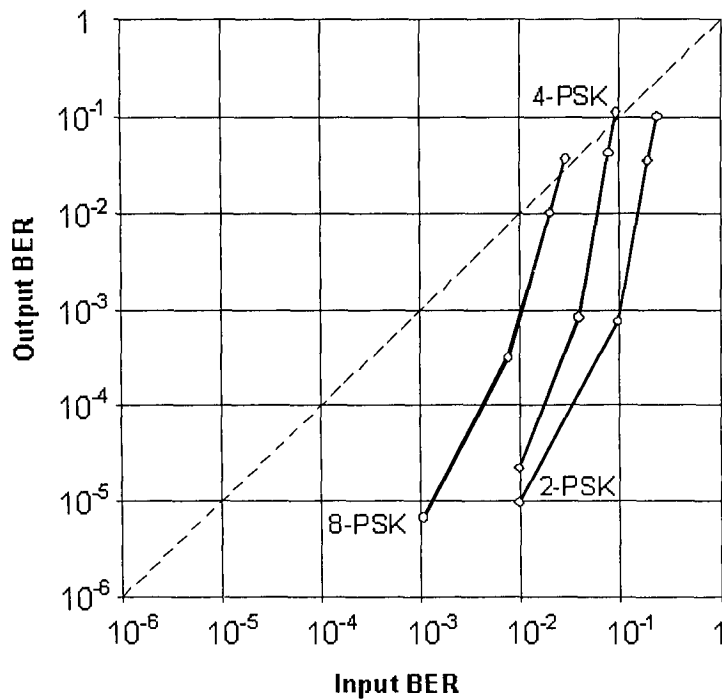


Figure 3: Details of the processing algorithm for the 4285 waveform.



The current version of error-correction decoder used in the 4285 algorithm consists of a short de-interleaver and a Viterbi hard-decision decoder. These functions are also performed by the C40 processor. The performance curves for the current version of the decoder for 2-, 4-, and 8-PSK are given in Figure 4. For example, for a 4-PSK encoded waveform with an input BER (after jamming suppression) of  $2 \times 10^{-2}$ , the decoded BER is about  $10^{-4}$ , which represents a substantial improvement and is sufficiently low for practical purposes. In practice, use of error-correction coding is recommended, especially in a hostile environment.



*Figure 4: Performance curves for the error-correcting decoder implementation in the current version of the 4285 algorithm.*

## 4.0 TEST ARRANGEMENT

Two test arrangements were used at different stages of testing: the laboratory setup and the over-the-air setup. They are described in the following subsections.

## 4.1 Laboratory Setup

The laboratory test is usually the first test of a real-time algorithm because it simulates an ideal propagation scenario. Instead of transmitting and receiving antennas, a network of radio-frequency (RF) cables is used to simulate communications and jamming signals incident on a receiving array from different directions. The baseband signals of the 4285 waveform and jamming signals must first be upconverted to the desired carrier frequency. A simple upconversion circuit was assembled with a combination of power splitters/combiners and mixers. Although this circuit produces both the upper and lower sidebands, the receivers were set to receive only the upper sideband, i.e. they were set to USB mode. A block diagram of the upconversion system is shown in Figure 5.

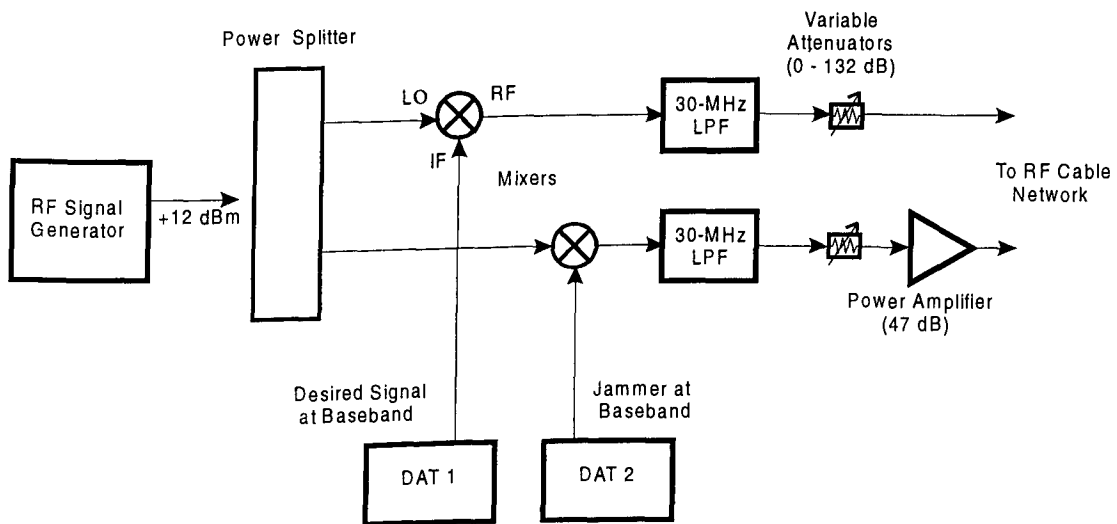


Figure 5: Diagram of the upconversion circuit for the desired signal and jammer.

The simulated signal scenario is shown in Figure 6. The array simulated is a linear array consisting of four equally spaced elements. The signal approaches the array from broadside; the jammer approaches at an angle  $\theta$  with respect to the array normal.

Figure 7 shows how the desired signal and jamming signal are combined to yield four output signals using the cable network. As shown in the figure, each of the input signals is split into four equal-power portions, using a one-to-four power splitter. After being split four ways, the desired signal portions are fed through four cables of equal length (1.6 m); this simulates the fact that the desired signal approaches the array from

broadside. The four jamming signals are fed through cables that increase in length incrementally such that the second cable introduces a delay  $d$ , the third  $2d$ , and the fourth  $3d$ . The four source signals are combined with the four jamming signals in the four power combiners. The output of each combiner is then fed into the RF inputs of the receivers.

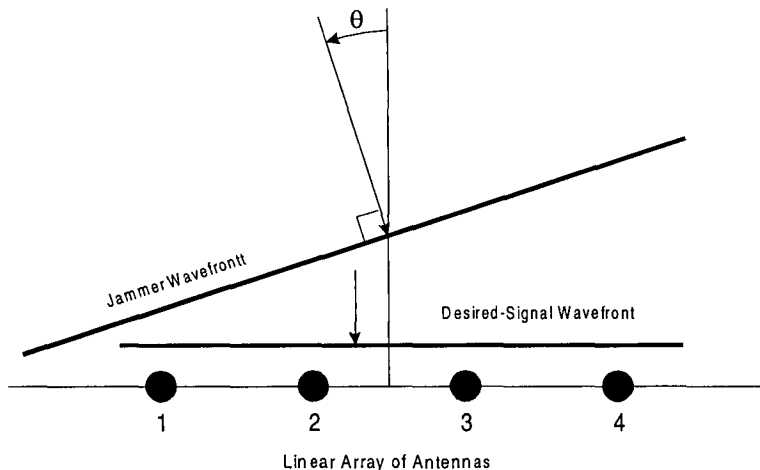


Figure 6: Simulated signal scenario for the laboratory tests.

The delay increments  $d$  used in the setup are 1.6 m of standard RG-58 cable. The relationship between incremental delay  $d$ , the assumed antenna spacing, and the angle of arrival of the jammer is straightforward to calculate. It can be shown, for example, that for  $d = 1.6$  m and an assumed antenna spacing of 5.0 m, the jammer direction is 27 degrees off broadside.

## 4.2 Over-the-Air Setup

The cable network provides an idealistic medium, for the measurements described above, in the sense that the signals entering the receivers are fully controlled. The powers and arrival directions of the desired signal and jammer are known, there are no multipath or Doppler-shift effects, and the thermal noise present at the receiver inputs is constant-power additive white Gaussian noise (AWGN). A real-world system uses antennas, for transmission and reception, in a much less ideal situation. Propagation through free space often comes with extraneous signals and noise, as well as distortion of the signals by the propagation medium and neighbouring objects along the path.

The over-the-air setup used four HF receiving antennas (Harris RF-1985) fed to the HFAARS, on the roof of Building 2 at CRC (Figure 8). These antennas are specifically

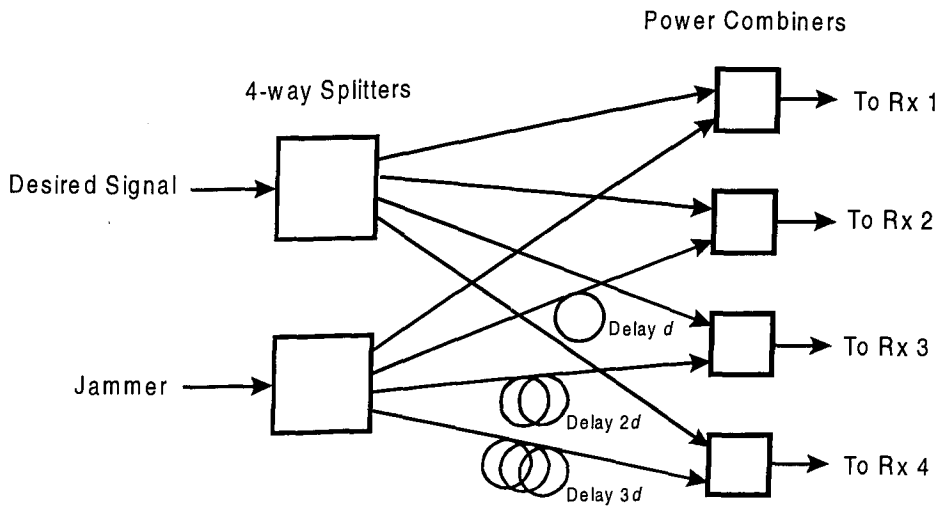


Figure 7: RF cable and splitter/combiner network to simulate the scenario of Figure 6.

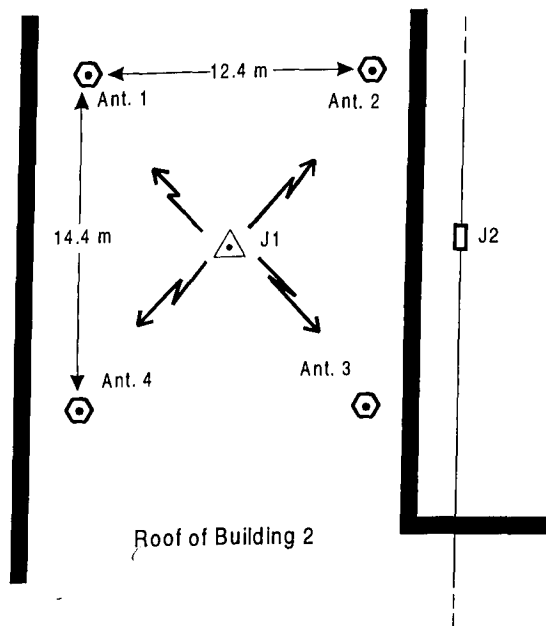
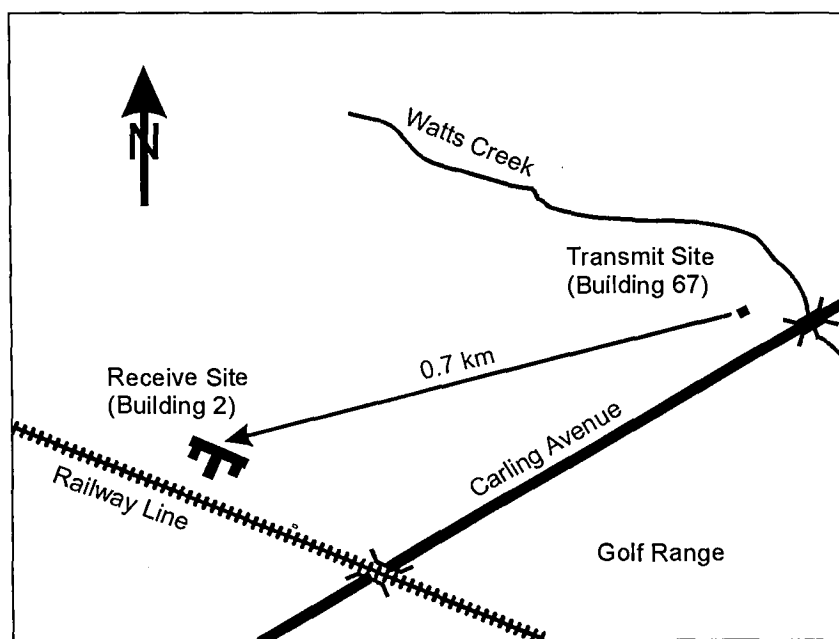


Figure 8: Bird's-eye view of the antenna layout on top of the northwest end of CRC's Building 2 (not to scale).

designed for shipboard installation. The jammer signal was produced by an upconversion using a double-balanced mixer as in Figure 5. It was fed to Antenna “J1”, a Harris RF-398 low-VHF vertical whip antenna located in the centre of the array. Antenna “J2” is a folded dipole about 26 m long suspended near the array; it was used at lower HF frequencies when Antenna “J1” was too inefficient to radiate sufficiently large jamming powers.

The desired signal was also upconverted by a double-balanced mixer, amplified, and transmitted from Building 67, about 0.7 km from Building 2 as shown in Figure 9. There is no obstruction between the two buildings. The transmitter RF source frequency and receiver tuned frequency were kept equal to well within 0.1 Hz by means of a rubidium 10-MHz reference source at the transmitter and a 10-MHz reference from a GPS receiver at the HFAARS.



*Figure 9: Layout for the over-the-air measurements at the CRC site.*

Note that the concept of planar wavefronts shown in Figure 6 is not applicable for the over-the-air system. For the jamming signal this is partly due to the fact that the jammer antennas are situated very close to the array in order to obtain high enough values of J/S with existing equipment. As well, both the desired-signal and the jammer-signal wavefronts are distorted because of reflections off the many metallic objects on the rooftop (e.g. other antennas, masts, catwalks, penthouses, metal stairways, roof flashing,



guy wires). These multipath components combine in a very complex way at the receiving antennas, much as occurs on a real ship. The rooftop also resembles a ship in that there is potential electromagnetic interference from transmissions at other frequencies, operation of heavy electrical equipment, lightning, etc.

Because of the proximity of the jammer antennas and multipath, the concept of a spatial null being formed by the algorithm is not applicable: there is no unique “direction” in which a null must be formed. However, for effective cancellation of interference, all that the algorithm requires is that the phases between the desired signal and the jamming signal differ by different amounts at each antenna, just as would occur if the signals came from afar, from different directions, and with no multipath. Thus, results of the over-the-air tests are very relevant to naval communications and better reflect how the algorithm would perform in a real-world environment. It is worth emphasizing that the algorithm does not require calibrated antennas, nor does it require a priori knowledge of the jammer direction.

## **5.0 SIGNAL TRANSMISSIONS**

Two types of signal transmissions are necessary: the communications (desired) signal and the jamming signal.

### **5.1 Communications Transmissions**

All 4285 signals were recorded on digital audio tapes (DAT) prior to the field trial. Each tape contained about one hour of a test message repeated continuously with a gap of five seconds between adjacent repetitions. The uncoded 4285 signals were originally generated by a computer simulation program developed at CRC based on the specification stated in [5]. The digital data were then loaded into the memory of an arbitrary waveform generator manufactured by Pragmatic, Model 2205A. Analog outputs from the Pragmatic waveform generator were recorded on the DAT tapes using a Sony digital audio recorder, Model PCM-7010. As the 4285 signal simulation program did not provide error-correction coded waveforms, coded 4285 signals were generated from a Harris modem, Model RF-5254C.

A block of ASCII text was used as the test message (Appendix A). The text contained 4074 ASCII characters or  $4074 \times 8 = 32\,592$  bits, including spaces. A four-byte end-of-message (EOM) mark, as specified in STANAG 4285, was attached to the end of each message.

A user interface on the HFAARS PC displayed the received text on the user monitor in real-time. A copy of the text was stored in the HFAARS PC for error-

monitoring purposes. Any character mismatch between the received text and the stored text was displayed as a flashing character on the monitor, indicating that one or more of the eight bits in that character were in error. At the end of each received message, a total bit-error count and corresponding BER were displayed on the monitor and recorded manually.

The transmit power was adjusted so that the SNR was approximately 20 dB. This is high enough to make the effects of incoherent noise, such as thermal noise, insignificant compared to the effects of the jammers.

## 5.2 Jamming Transmissions

The jamming signals used for these tests were generated using a jammer simulator developed at CRC. Jamming types included continuous noise, pulsed noise, and chirp.

The continuous-noise waveform was generated by software using a standard Gaussian random-noise generator, the NoiseCom Model NC-6101. The noise bandwidth was limited to approximately 5 kHz over the passband of the 4285 signal (before recording).

The pulsed-noise waveform was designed to yield near-optimal jamming effectiveness against the 4285 waveform, without the jamming noise pulse sequence being synchronized with the 4285 sequence. The jamming waveform consisted of a continuous train of random pulses, each pulse having a fixed width of 16 STANAG-4285 symbols, i.e. 6.7 ms. The interval between adjacent pulses was random with a mean interval of 48 symbols or 20 ms. A sample of the pulsed-noise waveform is shown in Figure 10. The extreme time variation of this jamming pulse train require the system to adapt rapidly and effectively even when only few symbols in each frame are jammed. More importantly, by virtue of their randomness, some of the jamming pulses fall in the message segment but not in the neighbouring known-reference segment of the 4285 signal. Under such circumstances, it is important that adaptation not be computed solely based on the known reference symbols, which might not be jammed. A unique anti-pulsed-jamming strategy was developed at CRC for this situation, and included in the 4285 algorithm. Use of this strategy does not degrade the system performance regardless of what jamming waveform is encountered. Details of this strategy are given in [2].

Chirp is a common waveform for jamming purposes because it can cover the entire bandwidth of the receiver, can provide a high-speed frequency-versus-time variation over a short period of time, and can be easily generated. The chirp waveform used for the trials was recorded on tape, with a sweep rate of 24 kHz/second over a 2.4-kHz range, corresponding to 10 sweeps/second (Figure 11).

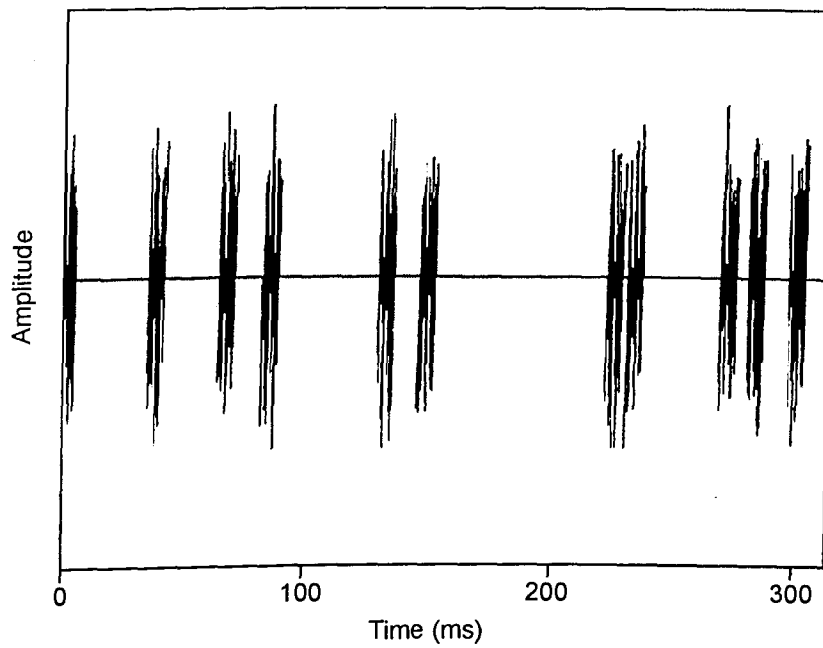


*Figure 10: A sample of the pulsed-noise jamming waveform.*

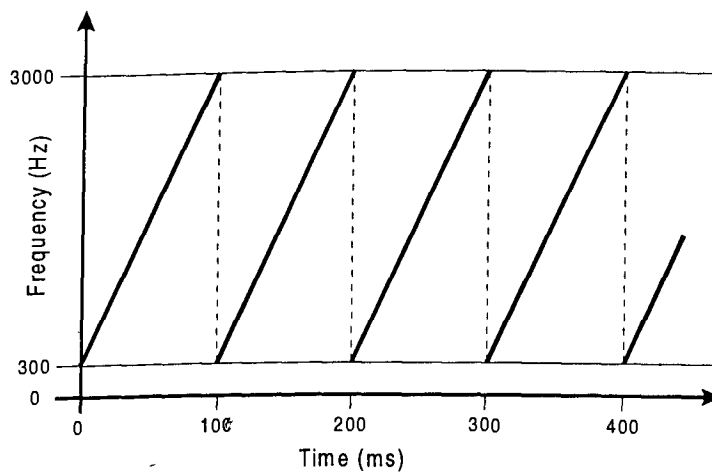


*Figure 11: Frequency-sweep characteristic of the chirp jamming waveform.*

Often the jamming power level was set to give the desired J/S by trial and error. The received power averaged over the four receivers was displayed on the HFAARS user interface. In the trial, the signal power S was measured with the jammer off; then the jammer was turned on and the measured total power (signal plus jammer) was taken as a measure of the jamming power J. In most cases, the jamming power was much stronger than the signal power (>10 dB) so that the latter measurement gave the jamming power sufficiently accurately. At lower J/S, the signal was turned off before the jammer power was measured.

## 6.0 TEST PARAMETERS

The operations and threat parameter selections used in the testing are summarized as follows:

Frequencies:	3.573, 7.01, 10.1 and 28.738 MHz
Signal modulation:	2-, 4- and 8-PSK
Error-correction coding:	coded and uncoded
Types of jamming signals:	continuous noise, chirp, and pulsed noise
Jamming-to-signal power ratios J/S:	0 to 50 dB, as well as no jamming

These result in a very large number of possible combinations which would take an unrealistically long time to evaluate. In this report, only results of representative performance are presented. Uncoded 4-PSK was used most often for the field trial and was taken as the benchmark for the 4285 signal. Using an uncoded signal gives a better evaluation of performance because all errors are revealed. Thus, as J/S is increased such that errors begin to occur, they are not masked by error correction. Jamming consisting of a single fixed tone was also tested; however, it was known a priori that this is the least harmful type of jamming for the algorithm and, indeed, tests confirmed this. Therefore tone jamming is not further discussed.

In practice, 4-PSK had a much better BER performance than 8-PSK for the following reasons:

1. The decision threshold for 8-PSK in the demodulation part of the algorithm is more stringent than 4-PSK because each symbol in 8-PSK carries 3 bits compared with 2 bits for 4-PSK.
2. The 8-PSK 4285 waveform employs a punctured error-correction-coding scheme with a rate of  $\frac{2}{3}$  instead of  $\frac{1}{2}$  which reduces the effectiveness of the error correction.

Performance curves for the decoders are shown in Figure 4.

In addition, it should be noted that the current anti-pulsed-jamming algorithm is more effective in 4-PSK than in 8-PSK. The anti-pulsed-jamming algorithm for 8-PSK had to be simplified in order to reduce the computation time in order to satisfy the real-time processing requirement [2]. The anti-pulse algorithm for 8-PSK can be improved when more processing power is available. This could be done by adding more C40 processors (only one was installed in the HFAARS) or using a faster processor in the TMS320C4x line. The speed of the C40 used for the present tests was 40 MHz, but at the time of writing, a 60-MHz version was available, a full 50% faster.

## 7.0 DATA PRESENTATION

The test data recorded were the number of bits in error for each repetition of the test message shown in Appendix A. Typically, several data points were taken at each value of  $J/S$ . These data are displayed in a set of charts of bit-error count and BER versus  $J/S$  (Appendix B). The 32 charts cover various operating conditions and ranges of signal and jamming types.

Each chart has two vertical-axis scales: the left scale represents the number of bit-error counts in the received message, and the right scale represents the corresponding BER, i.e. the number of bit errors divided by the total number of bits in the test message (32 592). The horizontal axis represents the input jamming-to-signal-power ratio ( $J/S$ ) in dB.

A single plotted point in the chart represents the error count and BER for one received message. Multiple measurements were taken (most often 5), and plotted at each  $J/S$  setting to quantify the error statistics, with different symbols used for the points.

The top horizontal line, labelled "Detection Failure", indicates cases when the system failed to detect the first or first few frames. This feature provides an indication of the likelihood of failure for the detection portion of the algorithm. The detection routine uses a decision threshold set by trial-and-error for groundwave propagation in the laboratory [2].

When a detection failure occurs, the system can still detect the remaining frames in the message. However, in the current user-interface monitoring routine, if the first or first few frames are missed, the rest of the received message is out of step with the reference text stored in the HFAARS, thereby invalidating the bit-error count.



## 8.0 RESULTS

The charts in Appendix B show the typical BER performance under various conditions as described below. Most of the tests do not use error-correction coding (these are marked "uncoded" in the caption) in order to evaluate the antijamming algorithm's performance in isolation, as discussed in Section 2.

### 8.1 4-PSK Signals (Charts 1 – 13)

#### 8.1.1 Continuous-Noise Jamming

Chart 1 shows the BER performance for a laboratory test using the cable network with continuous-noise jamming. The carrier frequency was set at 28.738 MHz. The result represents the best (lowest) BER achievable under an ideal propagation condition. There were no bit errors up to a J/S ratio of about 35 dB. Beyond a J/S ratio of 40 dB, the BER increased rapidly with J/S ratio mainly due to mismatches between the receivers [6].

Charts 2 - 4 show the BER performance for over-the-air tests with carrier frequencies set at 3.53, 7.01, and 10.1 MHz. The BERs are slightly higher than those in Chart 1. Overall, the BERs appear to be frequency-independent for the particular layout of the rooftop array. The spreads, of BER measurements for J/S between 30 and 40 dB, are larger than for the laboratory environment. This is most likely due to non-Gaussian or impulsive noise in the rooftop signal environment.

#### 8.1.2 Chirp Jamming

Charts 5 and 6 show the BER performance for chirp jamming in over-the-air tests. The results are similar to those for continuous-noise jamming.

#### 8.1.3 Pulsed-Noise Jamming

If noise jamming is pulsed rather than continuous, it can, for the same average power, cause higher BERs in adaptive-antenna systems. In particular, for the 4285 waveform, an intelligent jammer could jam only the known reference symbols but not the message symbols. This would cause the antijamming algorithm to calculate the weights while the jammer is off, leading to incorrect weights which in turn allows jamming to corrupt the message portion of the waveform. Although timing a jamming signal to achieve this jamming strategy perfectly is difficult, the jammer could transmit a pulse chain with random intervals, like the pulsed jamming waveform shown in Figure 10. Although imperfect (from the jammer's point of view) this jamming strategy could still be effective in disrupting the communications link. The result for a conventional adaptive receiver (i.e. with the anti-pulse feature turned off) in the presence of pulsed jamming is shown in Chart

7, where the BER approaches  $10^{-1}$ . The high BER shown in Chart 7 can be reduced by use of error-correction coding; the resulting BER performance is shown in Chart 8. Because of the high input BER, the output BER is still relative high, in the order of  $10^{-3}$  to  $10^{-2}$ .

The anti-pulsed-jamming feature described in [2] was designed to combat any type of pulsed jamming. When this feature is used in the absence of error correction (Charts 9 and 10), the BER level is reduced to less than  $10^{-3}$  for J/S ratios under 35 dB. The results of Charts 9 and 10 are for laboratory and over-the-air testing respectively, and may be compared with Charts 7 and 8 for which the anti-pulse feature was not used. The anti-pulse feature can be combined with error-correction coding to yield much lower BER in the presence of pulsed jamming (almost zero in most cases). The BER performance for pulsed, continuous-noise, and chirp jamming, with anti-pulse on and error-correction coding, is shown in Charts 11, 12 and 13, respectively.

It should be noted that although the anti-pulse feature is referred to as being “on” or “off”, in reality the former case means running a version of the antijamming algorithm without the anti-pulse feature, and the latter means running a different executable in which the algorithm includes the anti-pulse feature. On the basis of these findings, only the second one would be implemented in an operational system, since running the anti-pulse feature does not degrade the performance of the antijamming when other types of jammers are present.

## 8.2 8-PSK Signals (Charts 14 – 21)

Similar experiments were repeated for an 8-PSK 4285 waveform. As expected, an 8-PSK signal has a higher BER than its 4-PSK counterpart because each symbol carries one more bit. In addition, synchronization of the symbols becomes more critical. In the current version of the algorithm, the number of complex samples per symbol is four, the same as for 4-PSK and 2-PSK; this limits synchronization to an accuracy of  $1/8$  baud interval. In future versions of the algorithm, the number of samples per symbol should be increased to enhance the BER performance for 8-PSK.

The BER performance for continuous-noise and chirp jamming is shown in Charts 14 to 17, with carrier frequencies of 10.1 and 28.738 MHz. In these cases, the BERs tend to start off at about  $10^{-3}$ . The BER for pulsed-noise jamming (Chart 18) tends to start off at about  $10^{-2}$ . The worse BER performance is due to the use of a less effective but less computationally demanding anti-pulsed-jamming algorithm for 8-PSK, necessitated by the limited processing capability of the system [2].

Error-correction coding can be applied to lower the BER, as seen in Charts 19 - 21. For continuous-noise jamming and no error correction (Charts 14 and 15), the BER is flat at around  $10^{-3}$  from J/S = 0 to 40 dB; with coding (Chart 19), the BER is suppressed well below  $10^{-3}$ , in some cases to zero, over the same range of J/S.

Improvements also occurred for chirp jamming (Charts 16 and 17 vs. Chart 20) and pulsed-noise jamming (Chart 18 vs. Chart 21), although not as much as for continuous-noise jamming.

### **8.3 2-PSK Signals (Charts 22 – 24)**

BER performance for 2-PSK is much better than for 4-PSK and 8-PSK. For J/S less than about 24 dB, the BER is below  $10^{-4}$  for any type of jamming and carrier frequency. This is due to 2-PSK bearing only 1 bit per symbol or, equivalently, having more energy per bit than 4- and 8-PSK.

### **8.4 Performance Under Direct Control of Electrical Phase Angles of the Jamming Signals (Charts 25 – 32)**

The cable network shown in Figure 7 provided a constant incremental delay between jamming signals picked up by adjacent antennas. This was done to simulate a linear array with the jammer approaching at some physical angle. However, at the highest tested frequency, the resulting electrical-phase difference between adjacent jammer-signal cables was about 77.5 degrees. At lower frequencies, this value is proportionately lower.

In order, then, to better understand the behaviour of the antijamming algorithm over the full range of possible electrical-phase differences in adjacent antennas, a different setup was used: the delay lines of Figure 7 were replaced by phase shifters used at their operating frequency of 30 MHz. A series of BER measurements was made using the 4-PSK signal and continuous-noise jamming. Results for selected phase increments are shown in the charts.

Chart 25 shows the results of BER measurements with zero degrees of phase difference between adjacent-antenna jamming signals. This corresponds to having the jammer directly in line with the desired signal. Under these conditions, the algorithm cannot suppress the jammer, and performance is understandably poor.

Chart 26 shows the result with 5-degree incremental phase shift, i.e. the jamming signal in Receiver 2 was 5 degrees behind that in Receiver 1, the jamming signal in Receiver 3 was 10 degrees behind that in Receiver 1, and the jamming signal in Receiver 3 was 15 degrees behind. This corresponds to a real-world situation in which the direction of the jammer is close to that of the desired signal. There is some improvement in the BER. As the incremental phase is increased up to 180 degrees, the BER performance improves. The best performance is seen to be at 180 degrees. Results for phase increments beyond 180 degrees are “reflections” of those below 180 degrees, so that at phase increments of 360 degrees, the result is identical to that at 0 degrees.

The results for all the measurements are summarized in Figure 12. Here we plot the maximum  $J/S$  for which the BER is less than approximately  $10^{-3}$ . The plot confirms the rule of thumb that in practical systems the array elements should be spaced at least one-quarter wavelength apart. Under this condition, the likelihood that the electrical phase differences for the desired signal and jammer, within each antenna element, are sufficiently different to permit effective interference cancellation. Of course, when the desired signal and jammer are collinear, the jammer and desired-signal phases in each element differ by the same amount and no nulling is possible.

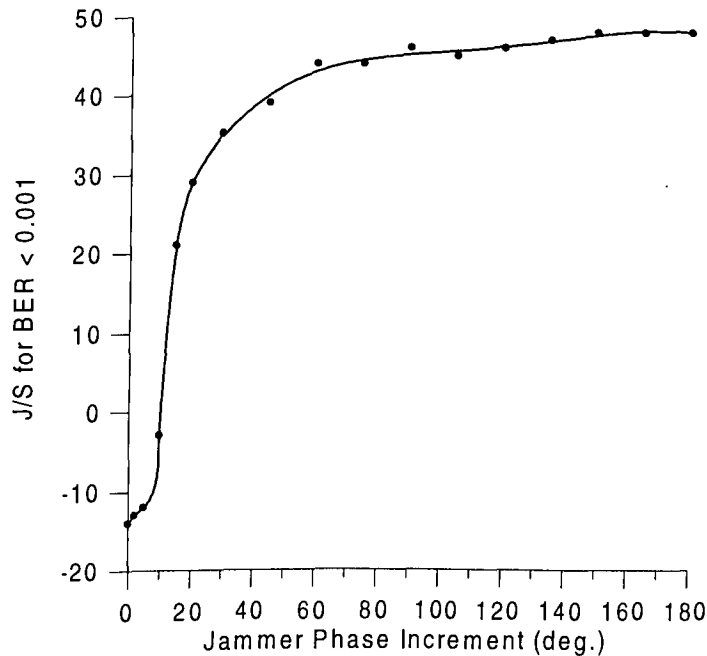


Figure 12: Plot of maximum  $J/S$  for BER less than  $10^{-3}$ , as a function of jammer phase increment.

## 8.5 Multiple Jammers

In theory, a four-element array can null out up to three independent jammers. At the time the present measurements were made it was confirmed, in a very limited number of trials, that two independent jammers could be suppressed by as much as if only one were on at a time. More detailed measurements on multiple jammers were made using the same antijamming algorithm in the PHFARS. Those results are beyond the scope of this report, but are described in [4]. In general, for two and three jammers there was excellent jamming suppression that was only slightly worse than for a single jammer. For example,

in one instance when continuous-noise, chirp, and pulsed-noise jammers were simultaneously incident, the BER remained below  $10^{-2}$  for total-jammer-to-signal ratio of up to 35 dB.

## 9.0 CONCLUSIONS

The reported measurements prove that the anti-pulse version of the STANAG 4285 antijamming algorithm performs excellently over a wide range of parameters. The tests covered most of the HF band – from 3.53 to 28.738 MHz, and were done using both a laboratory RF scenario simulator and locally over the air. The jammer types used were broadband noise, pulsed noise, and chirp. The results were essentially independent of the frequency and can be summarized as follows:

1. For 2- and 4-PSK modulation, BER of less than  $10^{-3}$  were obtained, for J/S up to at least 30 dB and in some instances to 40 dB.
2. When the error-correcting mode of the 4285 waveform for 2- and 4-PSK was used, low post-correction values of BER were obtained for J/S up to at least 45 dB — a power ratio of over 30,000.
3. The performance of 8-PSK was worse than for 2- and 4-PSK: typically the uncoded form produced an error rate of  $10^{-3}$  for J/S = 30 dB down to 0 dB.

Future versions of the algorithm should increase the number of samples per symbol interval to compensate for the poorer performance for 8-PSK. This will require another C40 DSP processor to handle the additional processing demands.

The most important implication of the test results is that the large reduction of J/S achieved by the algorithm can render brute-force jamming ineffective.

Finally, it should be noted that the DSP techniques described herein do not depend on the signals' carrier frequency. Similar techniques can therefore be used at higher frequencies, in particular at current mobile communications frequencies in the VHF and UHF bands.

## ACKNOWLEDGEMENTS

This work was sponsored by the Department of National Defence (DMSS 8) as part of the research on adaptive-antenna signal processing techniques.

## REFERENCES

1. K. H. Wu, "*Design of a VXibus-based Programmable HF Adaptive Receiving System (PHFARS)*", report in preparation, 1997.
2. K. H. Wu, "*Adaptive-Antenna Signal Processing Techniques and Implementation for the NATO STANAG 4285 Waveform*", CRC Report No. CRC-RP-97-003, August 1997.
3. Lt(N) M. Craig, "*Interference Suppression Using an HF Adaptive Antenna Receiving System (HFAARS)*", Maritime Engineering Journal, June 1995, pp. 20-22.
4. A. Tenne-Sens, "*Performance Evaluation of the Programmable HF Adaptive Receiving System (PHFARS) for the NATO STANAG 4285 Waveform in a Jamming Environment*", CRC Report No. CRC-RP-97-005, December 1997.
5. Military Agency for Standardization (MAS), North Atlantic Treaty Organization (NATO), "*Standardization Agreement, STANAG 4285 (2nd draft, Edition 1)*" (originally classified as NATO RESTRICTED, declassified to UNCLASSIFIED on 9 Feb. 1993).
6. K. H. Wu, "*Digital Matching of Receivers for an Adaptive-Antenna Receiving System*", CRC Technical Note No. 02/97, January 1997.



## APPENDIX A: THE TEST MESSAGE

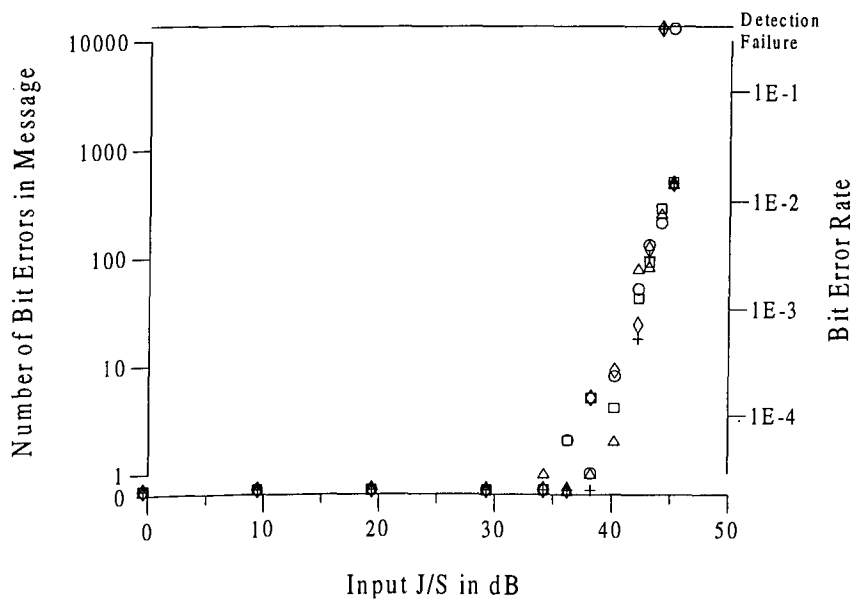
It was the best of times, it was the worst of times, it was the age of wisdom, it was the age of foolishness, it was the epoch of belief, it was the epoch of incredulity, it was the season of Light, it was the season of Darkness, it was the spring of hope, it was the winter of despair, we had everything before us, we had nothing before us, we were all going direct to Heaven, we were all going direct the other way - in short, the period was so far like the present period, that some of its noisiest authorities insisted on its being received, for good or for evil, in the superlative degree of comparison only. There were a king with a large jaw and a queen with a plain face, on the throne of England; there were a king with a large jaw and a queen with a fair face, on the throne of France. In both countries it was clearer than crystal to the lords of the State preserves of loaves and fishes, that things in general were settled for ever. It was the year of Our Lord one thousand seven hundred and seventy-five. Spiritual revelations were conceded to England at that favoured period, as at this. Mrs. Southcott had recently attained her five-and-twentieth blessed birthday, of whom a prophetic private in the Life Guards had heralded the sublime appearance by announcing that arrangements were made for the swallowing up of London and Westminster. Even the Cock-lane ghost had been laid only a round dozen of years, after rapping out its messages as the spirits of this very year last past (supernaturally deficient in originality) rapped out theirs. Mere messages in the earthly order of events had lately come to the English Crown and People, from a congress of British subjects in America: which, strange to relate, have proved more important to the human race than any communications yet received through any of the chickens of the Cock-lane brood. France, less favoured on the whole as to matters spiritual than her sister of the shield and trident, rolled with exceeding smoothness down hill, making paper money and spending it. Under the guidance of her Christian pastors, she entertained herself, besides, with such humane achievements as sentencing a youth to have his hands cut off, his tongue torn out with pincers, and his body burned alive, because he had not kneeled down in the rain to do honour to a dirty procession of monks which passed within his view at a distance of some fifty or sixty yards. It is likely enough that, rooted in the woods of France and Norway, there were growing trees, when that sufferer was put to death, already marked by the Woodman, Fate to come down and be sawn into boards, to make a certain movable framework with a sack and a knife in it, terrible in history. It is likely enough that in the rough outhouses of some tillers of the heavy lands adjacent to Paris, there were sheltered from the weather that very day, rude carts, bespattered with rustic mire, snuffed about by pigs, and roosted in by poultry, which the Farmer, Death, had already set apart to be his tumbrils of the Revolution. But that Woodman and that Farmer, though they work unceasingly, work silently, and no one heard them as they went about with muffled tread; the rather, forasmuch as to entertain any suspicion that they were awake, was to be atheistical and traitorous. In England, there was scarcely an amount of order and protection to justify much national boasting. Daring burglaries by armed men, and highway robberies, took place in the capital itself every night; families were publicly cautioned not to go out of town without removing their furniture to upholsterers' warehouses for security; the highwayman in the dark was a City tradesman in the light, and, being recognized and challenged by his fellow-tradesman, whom he stopped in his character of "the Captain," gallantly shot him through the head and rode away; the mail was waylaid by seven robbers, and the guard shot three dead, and then got shot dead himself by the other four, "in consequence of the failure of his ammunition": after which the mail was robbed in peace. Ke<sup>2</sup>





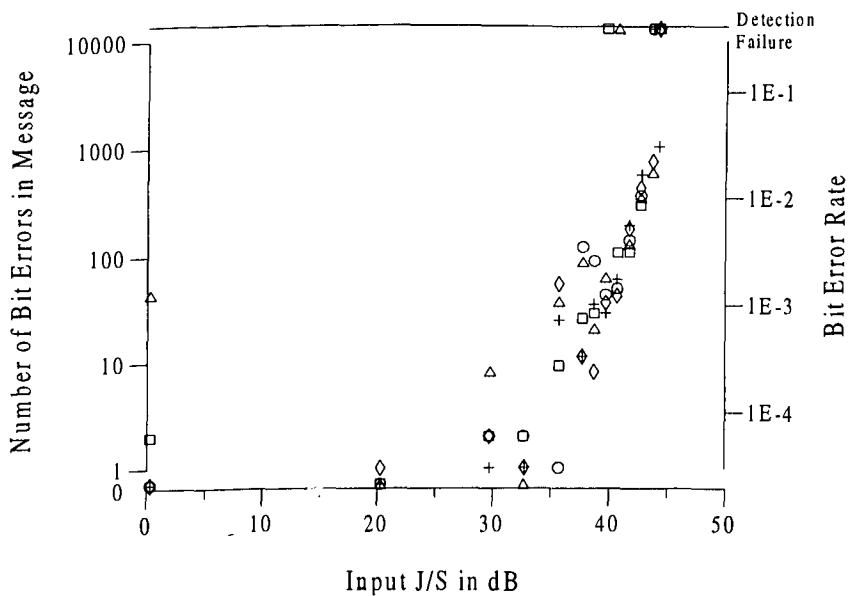
## APPENDIX B: TEST RESULTS

(In all the tests below, the anti-pulsed-jamming feature was used unless otherwise noted.)



4PJ4-1

Chart 1: 4-PSK, continuous-noise jamming, 28.738 MHz, laboratory test, uncoded.



4PJ4-3

Chart 2: 4-PSK, continuous-noise jamming, 3.53 MHz, over-the-air test, uncoded.

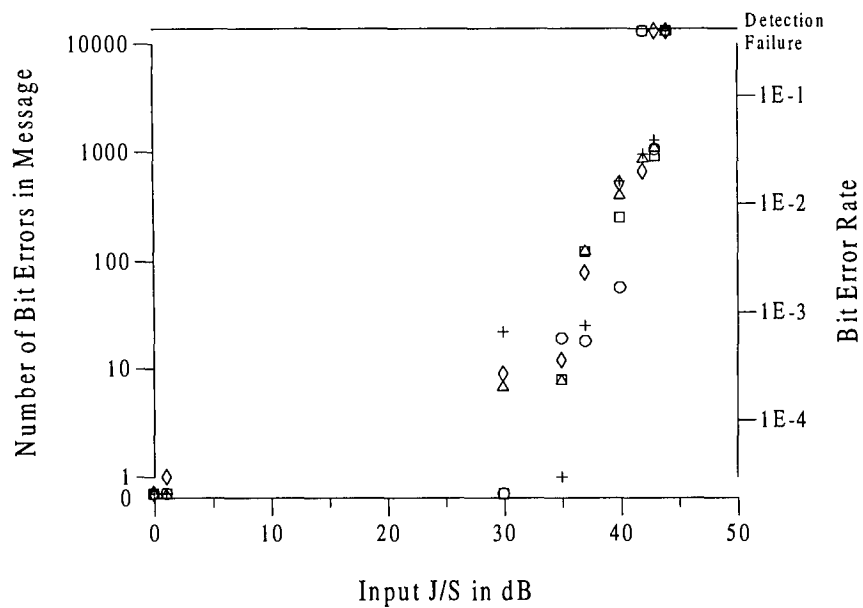


Chart 3: 4-PSK, continuous-noise jamming, 7.01 MHz, over-the-air test, uncoded.

4PJ4-4

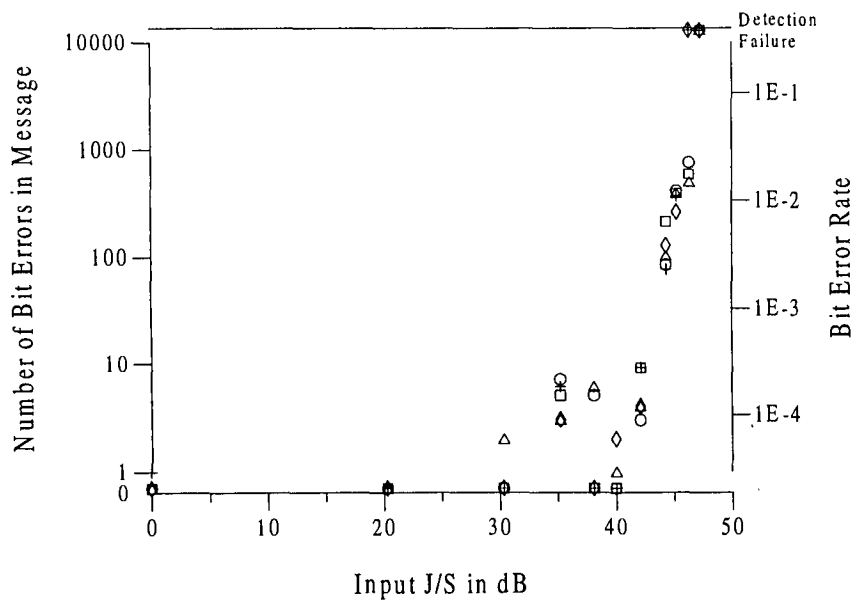
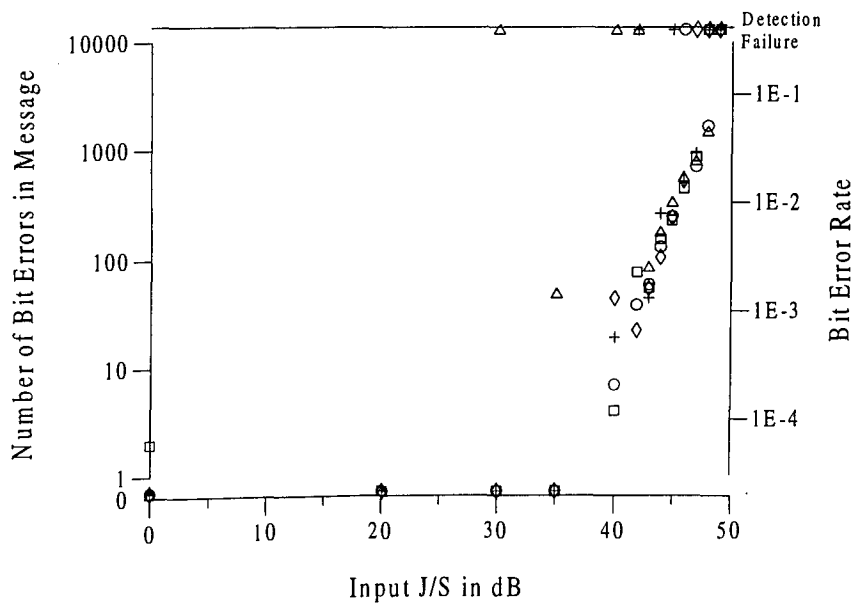


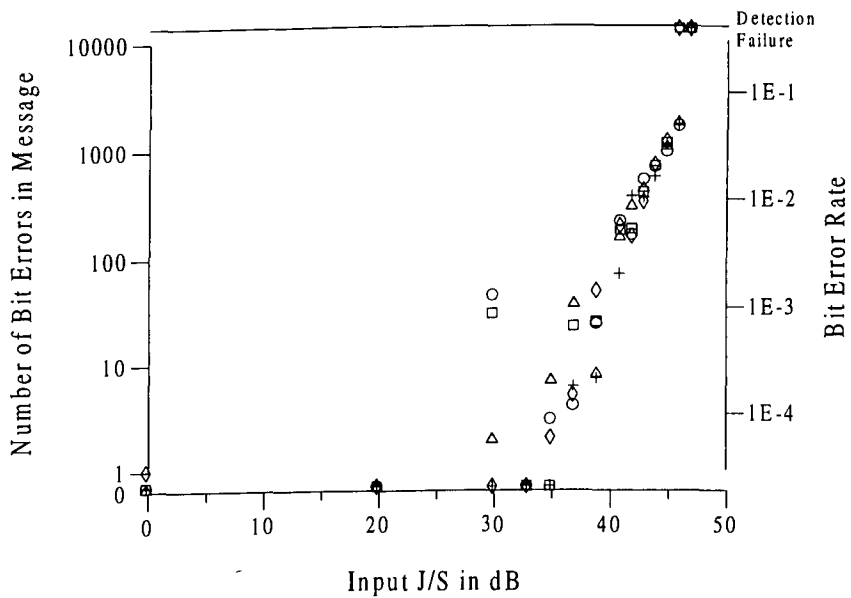
Chart 4: 4-PSK, continuous-noise jamming, 10.1 MHz, over-the-air test, uncoded.

4PJ4-5



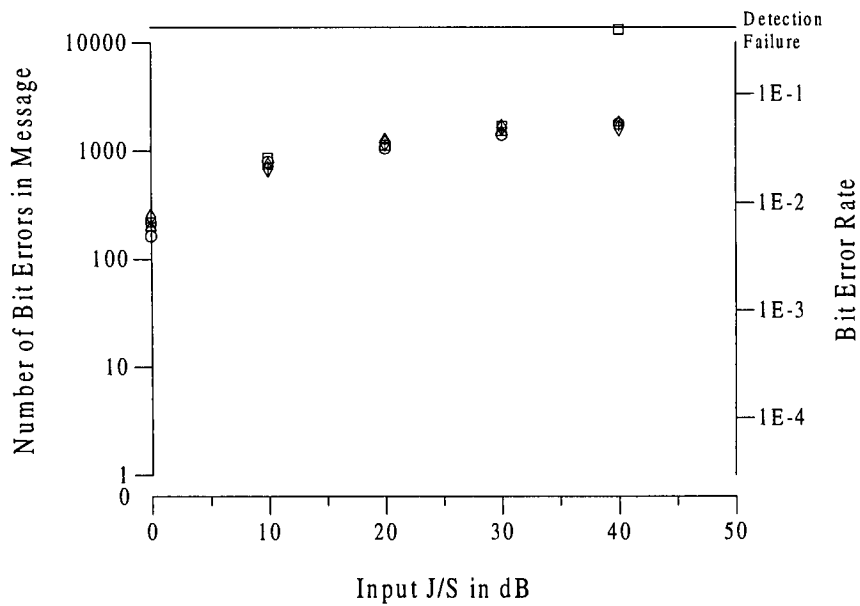
4PJ5-4

Chart 5: 4-PSK, chirp jamming, 10.1 MHz, over-the-air test, uncoded.



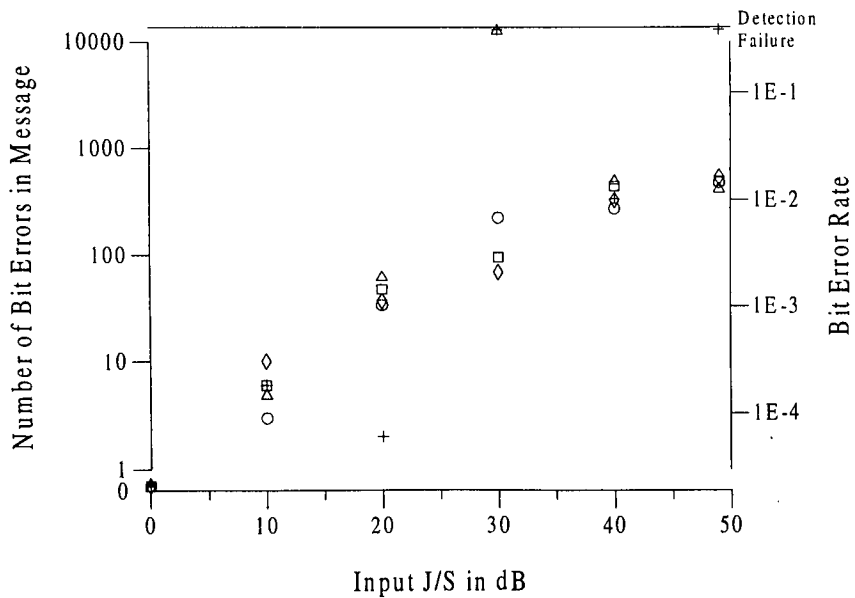
4PJ5-2

Chart 6: 4-PSK, chirp jamming, 7.01 MHz, over-the-air test, uncoded.



4J6-2

Chart 7: 4-PSK, pulsed-noise jamming, 10.1 MHz, over-the-air test, anti-pulse off, uncoded.



4CJ6-3

Chart 8: 4-PSK, pulsed-noise jamming, 10.1 MHz, over-the-air test, anti-pulse off, coded.

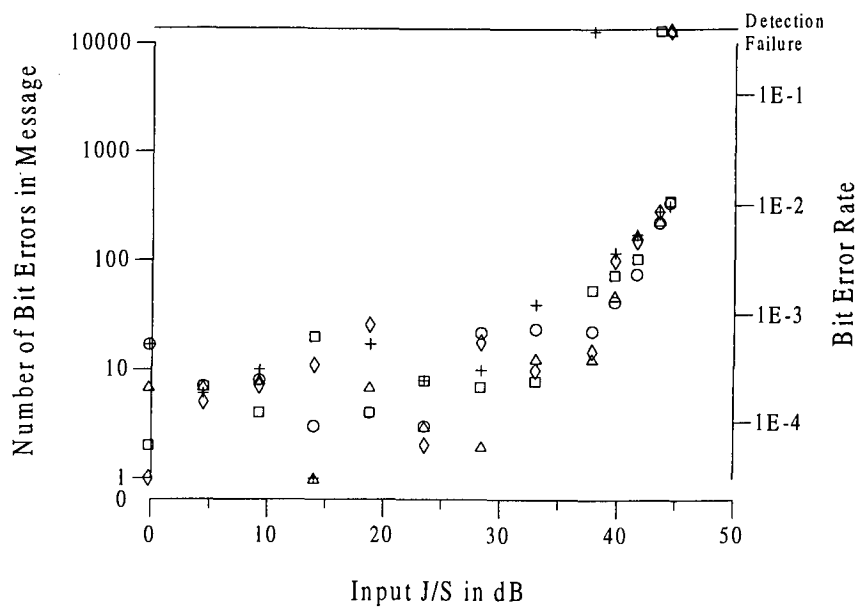


Chart 9: 4-PSK, pulsed-noise jamming, 28.738 MHz, laboratory test, uncoded. 4PJ6-1

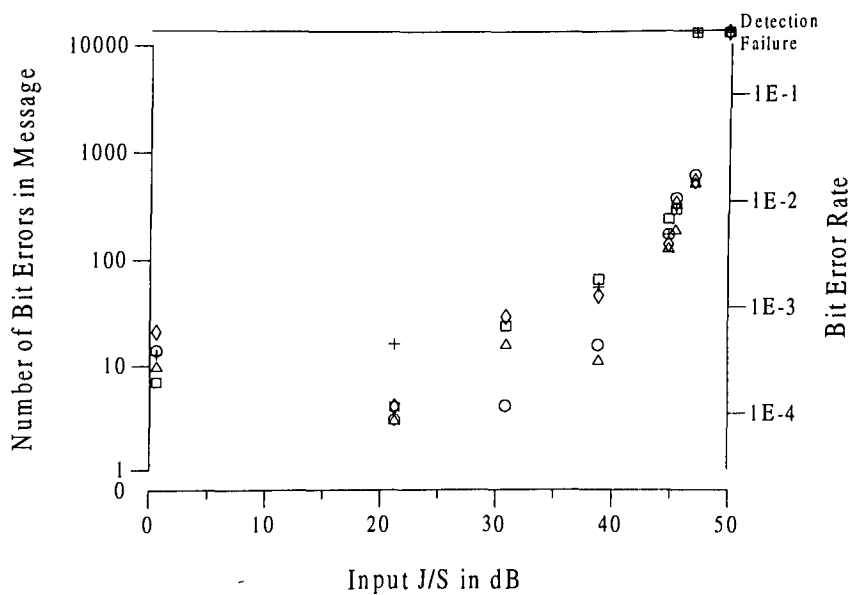


Chart 10: 4-PSK, pulsed-noise jamming, 28.738 MHz, over-the-air test, uncoded. 4PJ6-5

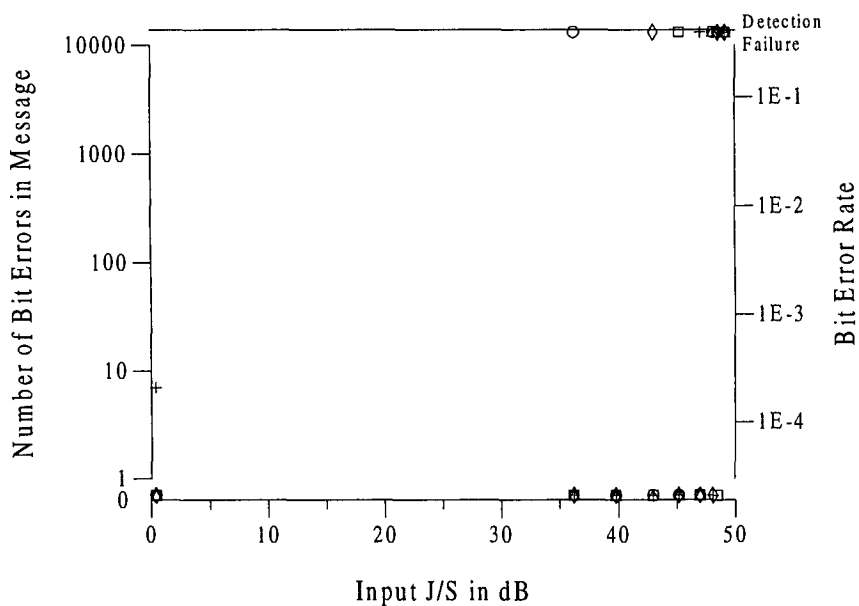


Chart 11: 4-PSK, pulsed-noise jamming, 28.738 MHz, over-the-air test, coded.

4PCJ6-5

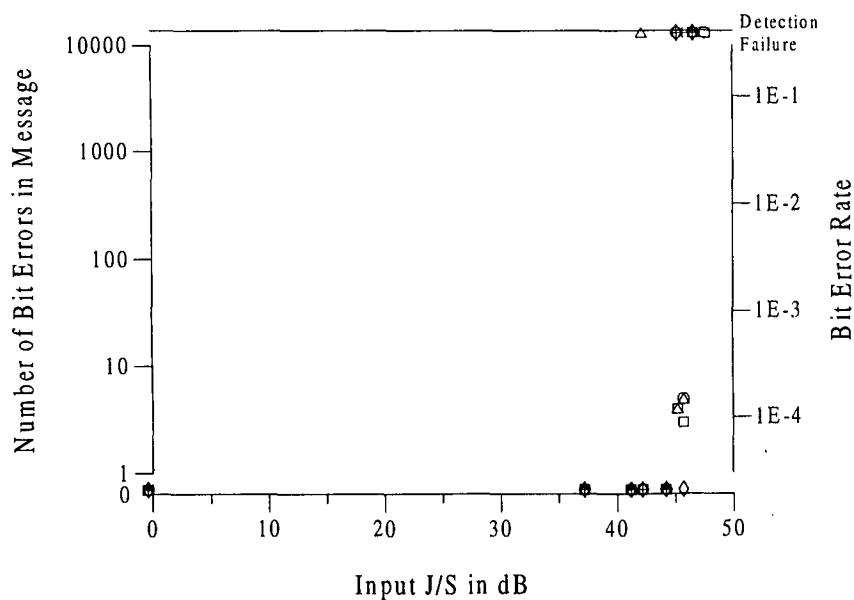
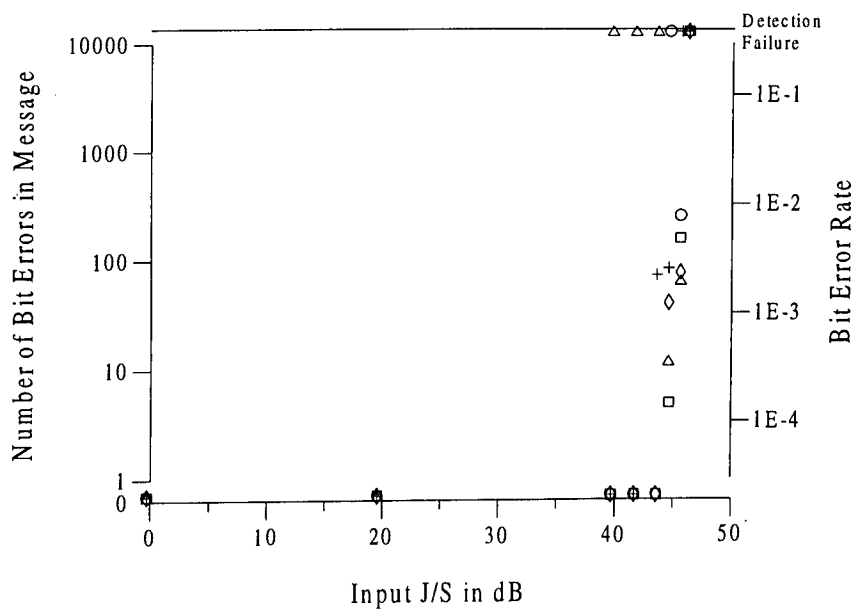


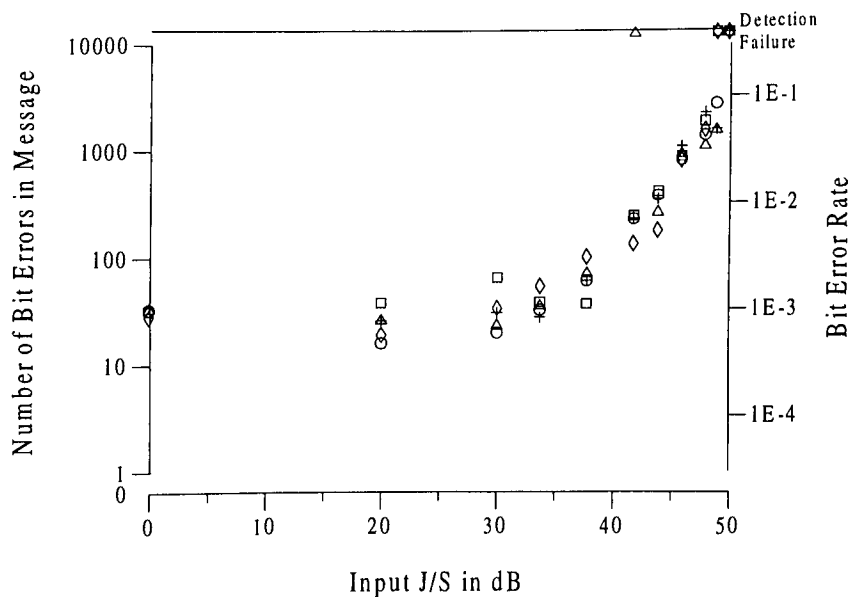
Chart 12: 4-PSK, continuous-noise jamming, 28.738 MHz, over-the-air test, coded.

4PCJ4-5



4PCJ5-5

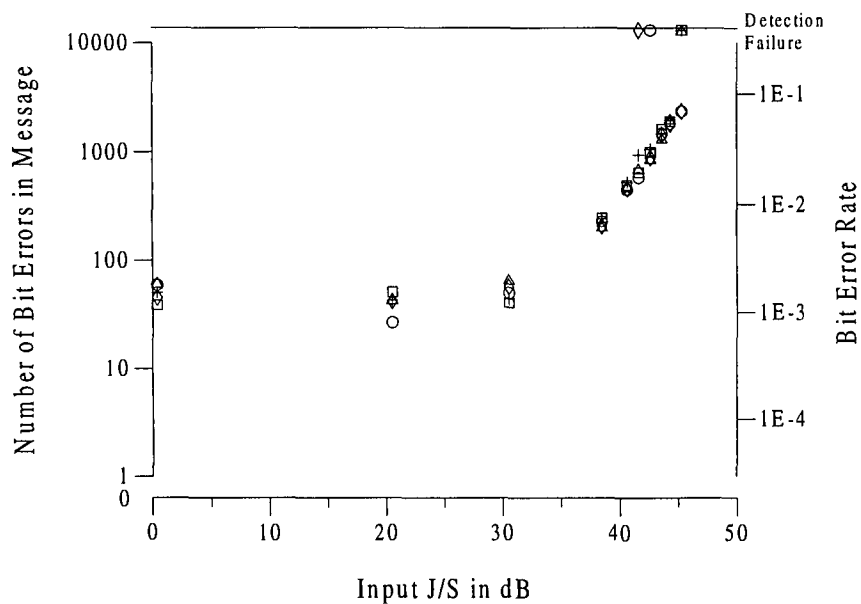
Chart 13: 4-PSK, chirp jamming, 28.738 MHz, over-the-air test, coded.



8PJ4-4

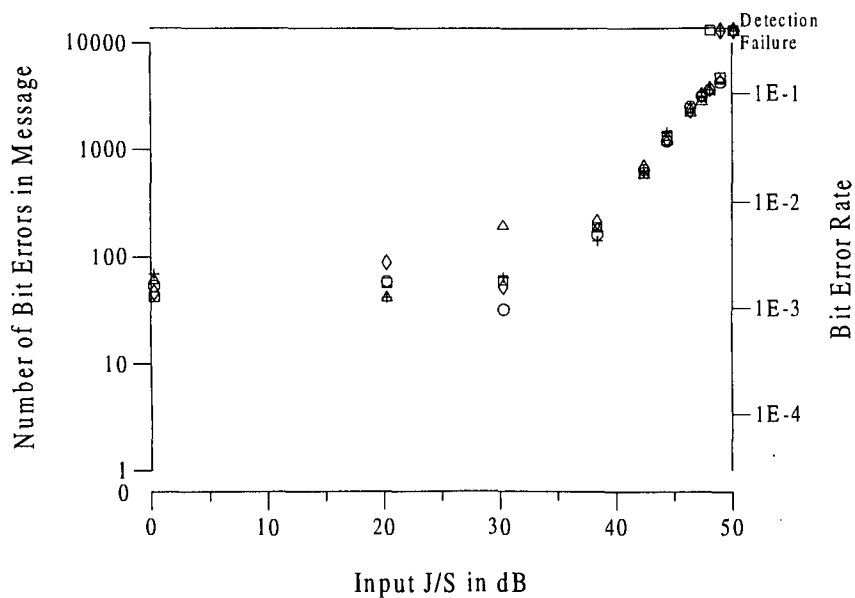
Chart 14: 8-PSK, continuous-noise jamming, 10.1 MHz, over-the-air test, uncoded.





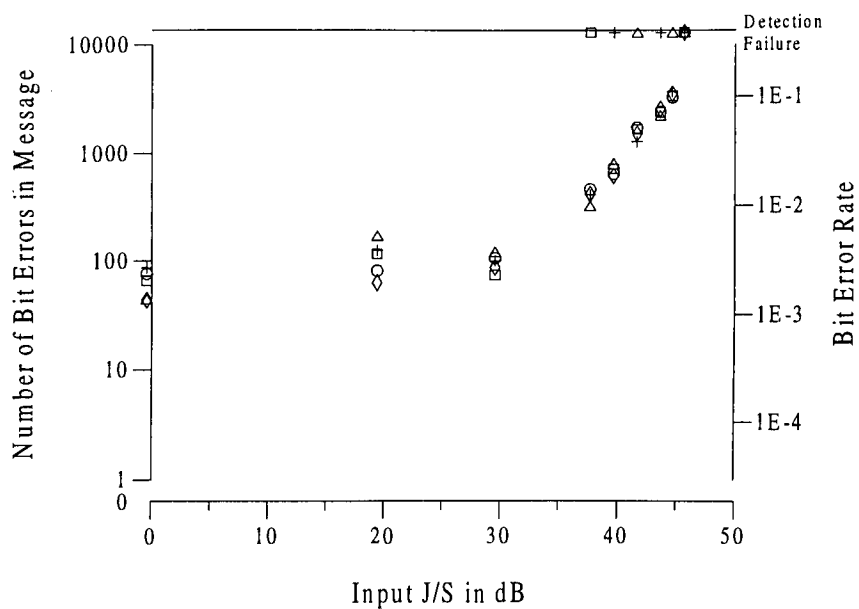
8PJ4-5

Chart 15: 8-PSK, continuous-noise jamming, 28.738 MHz, over-the-air test, uncoded.



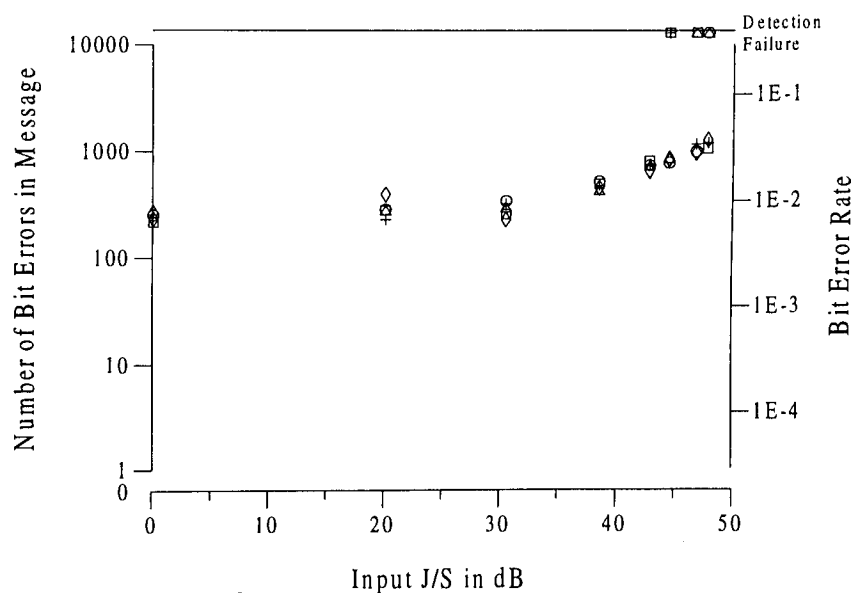
8PJ5-4

Chart 16: 8-PSK, chirp jamming, 10.1 MHz, over-the-air test, uncoded.



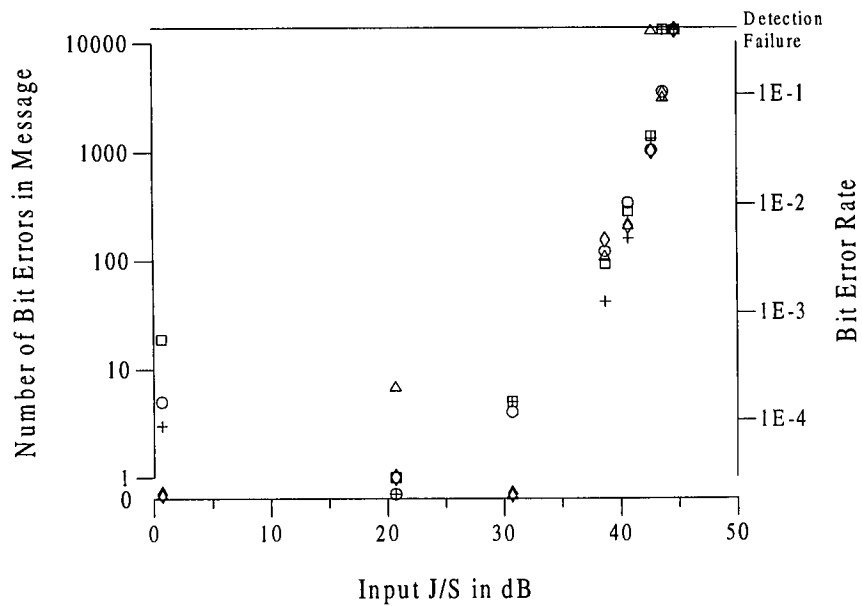
8PJ5-5

Chart 17: 8-PSK, chirp jamming, 28.738 MHz, over-the-air test, uncoded.



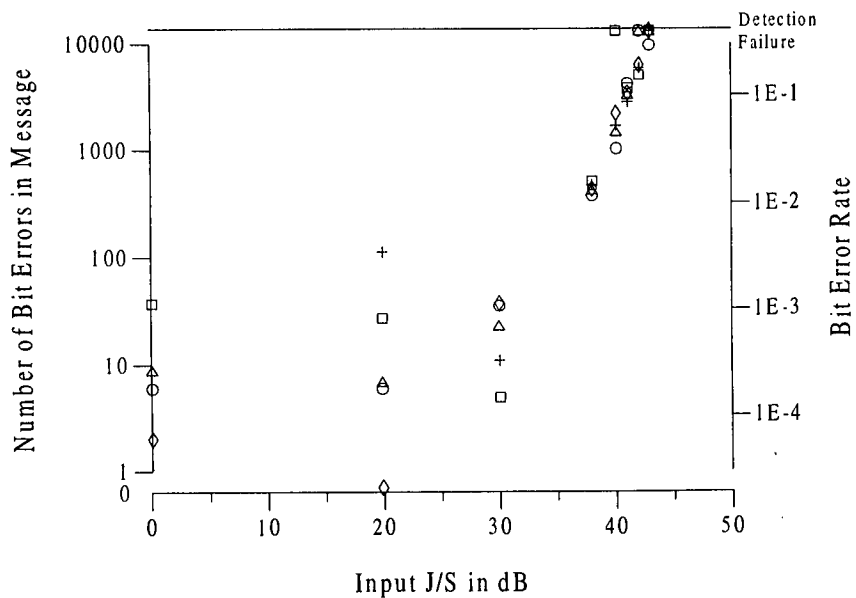
8PJ6-5

Chart 18: 8-PSK, pulsed-noise jamming, 28.738 MHz, over-the-air test, uncoded.



8PCJ4-5

Chart 19: 8-PSK, continuous-noise jamming, 28.738 MHz, over-the-air test, coded.



8PCJ5-7

Chart 20: 8-PSK, chirp jamming, 28.738 MHz, over-the-air test, coded.

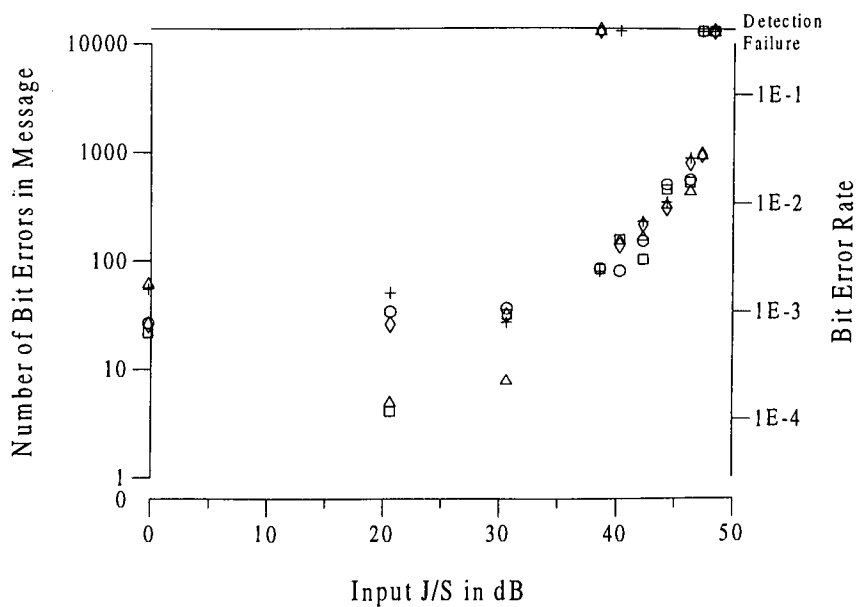


Chart 21: 8-PSK, pulsed-noise jamming, 28.738 MHz, over-the-air test, coded.

8PCJ6-6

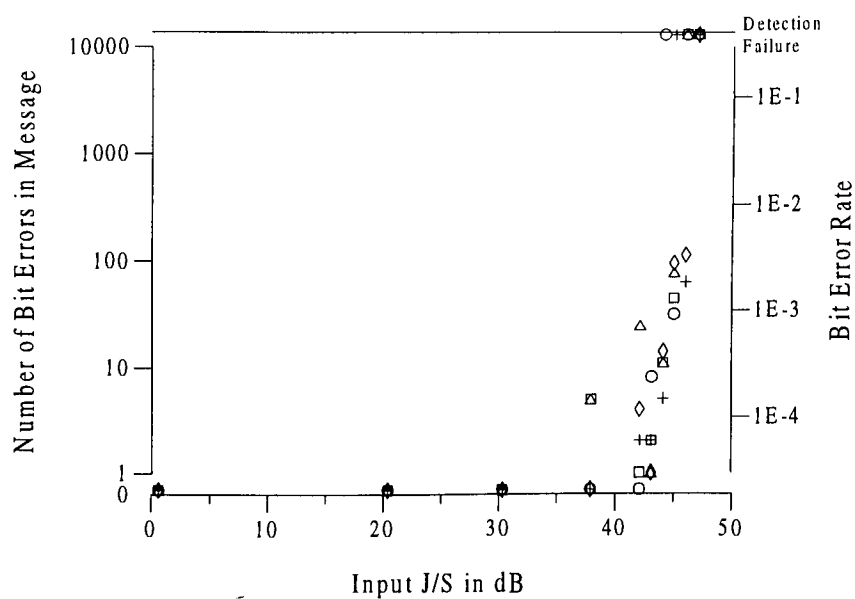


Chart 22: 2-PSK, continuous-noise jamming, 3.573 MHz, over-the-air test, uncoded.

2PJ4-2

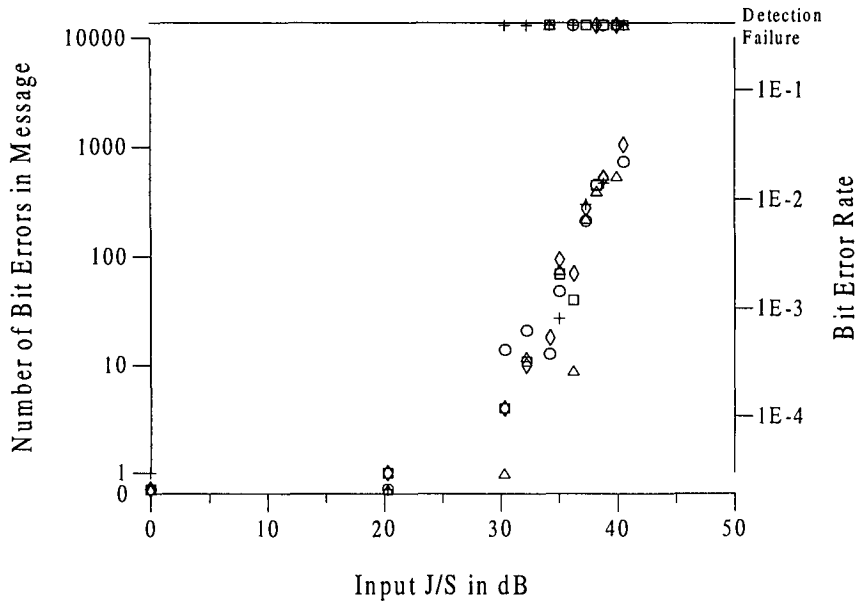


Chart 23: 2-PSK, chirp jamming, 3.573 MHz, over-the-air test, uncoded.

2PJ5-2

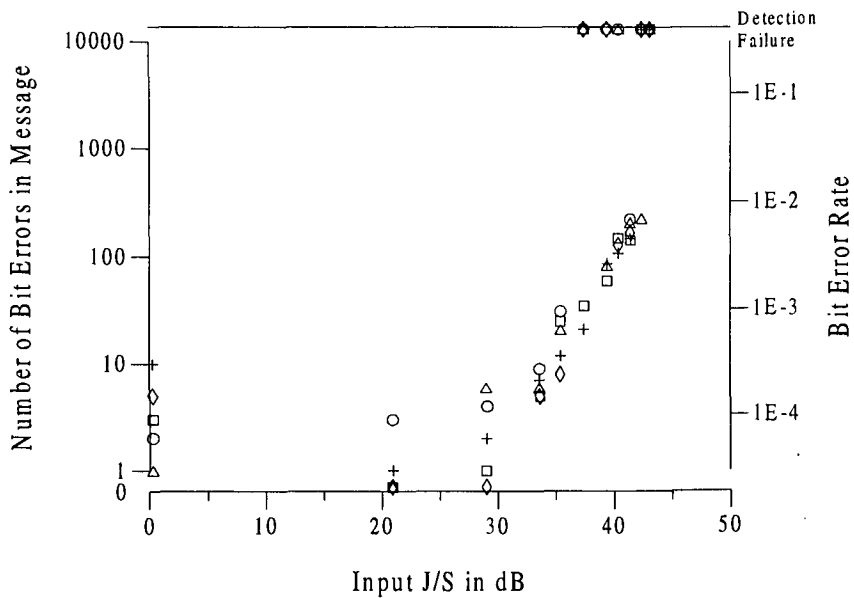
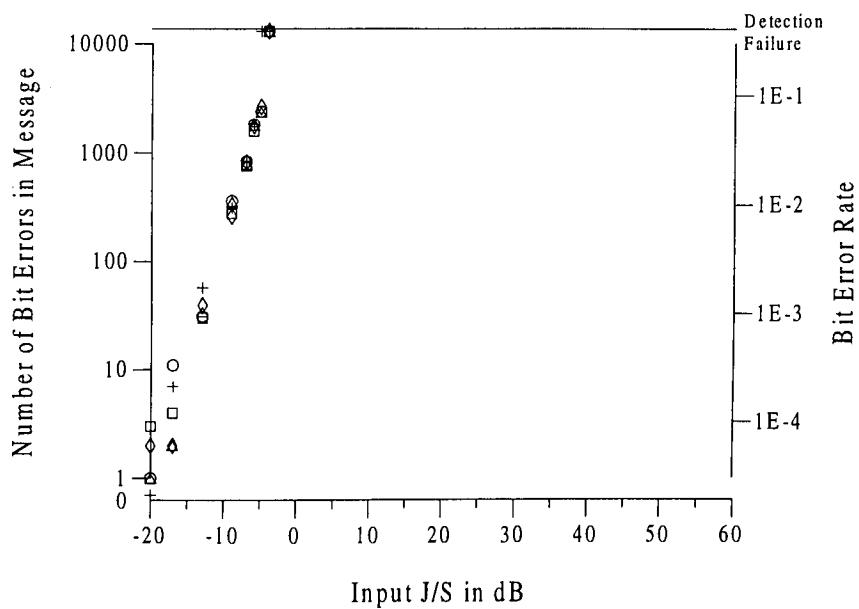


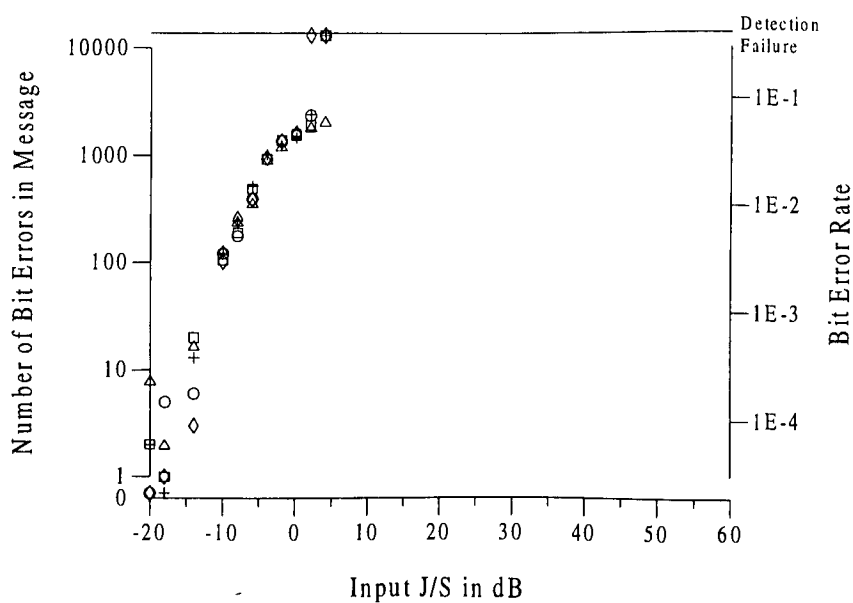
Chart 24: 2-PSK, pulsed-noise jamming, 3.573 MHz, over-the-air test, uncoded.

2PJ6-2



4PJ4-08

Chart 25: 4-PSK, continuous-noise jamming, 28.738 MHz, laboratory test, 0-degree jammer phase increments, uncoded.



4PJ4-10

Chart 26: 4-PSK, continuous-noise jamming, 28.738 MHz, laboratory test, 5-degree jammer phase increments, uncoded.

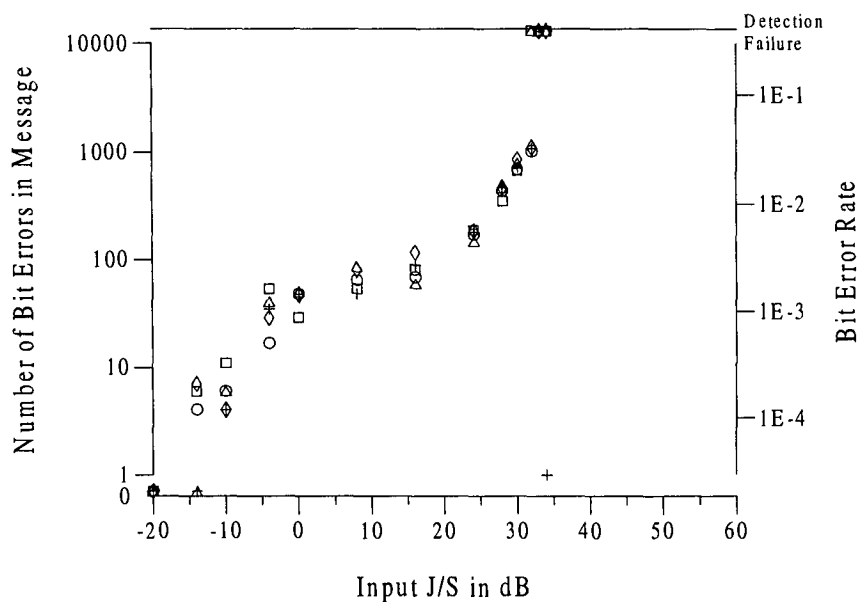


Chart 27: 4-PSK, continuous-noise jamming, 28.738 MHz, laboratory test, 10-degree jammer phase increments, uncoded.

4PJ4-11

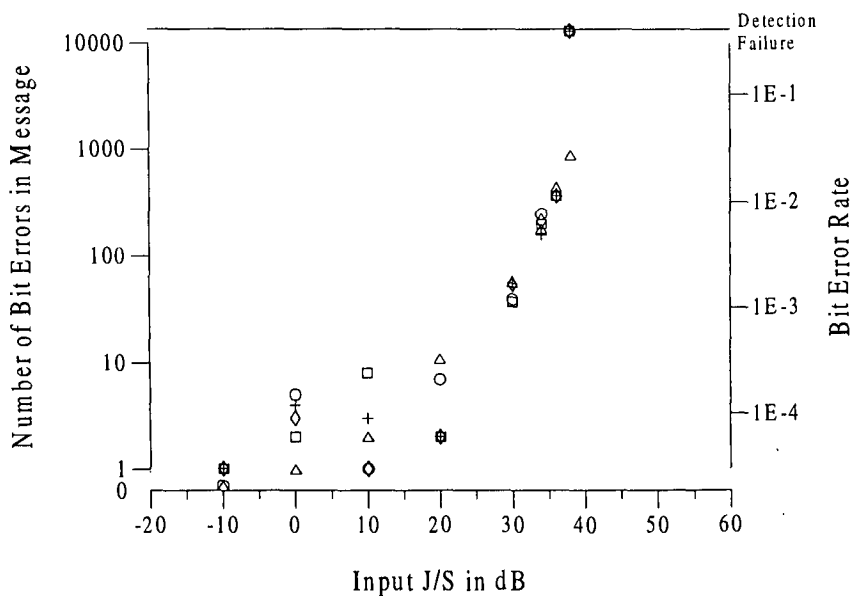
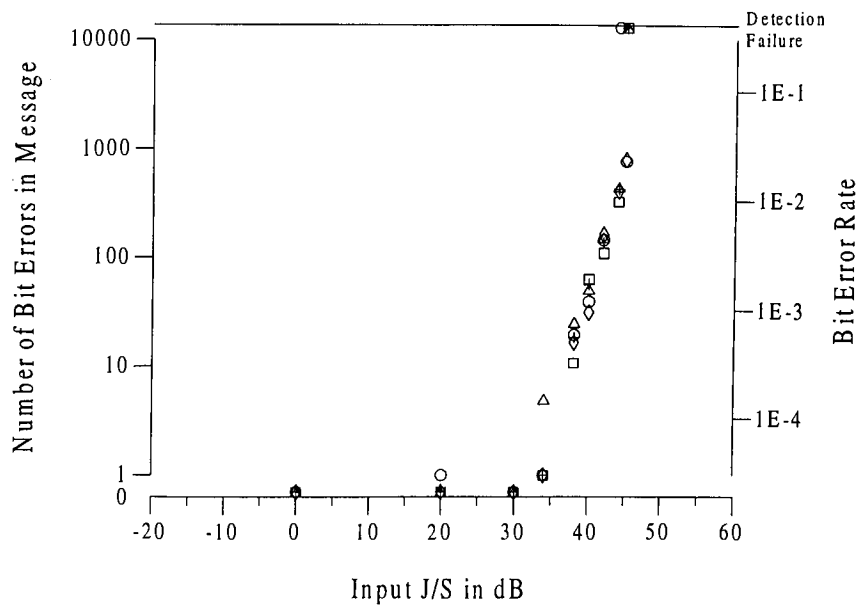


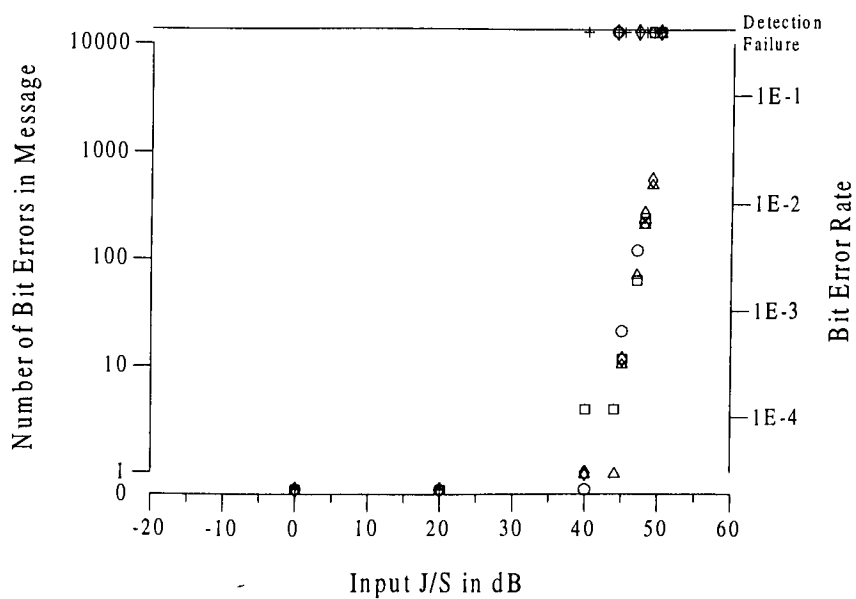
Chart 28: 4-PSK, continuous-noise jamming, 28.738 MHz, laboratory test, 20-degree jammer phase increments, uncoded.

4PJ4-13



4PJ4-15

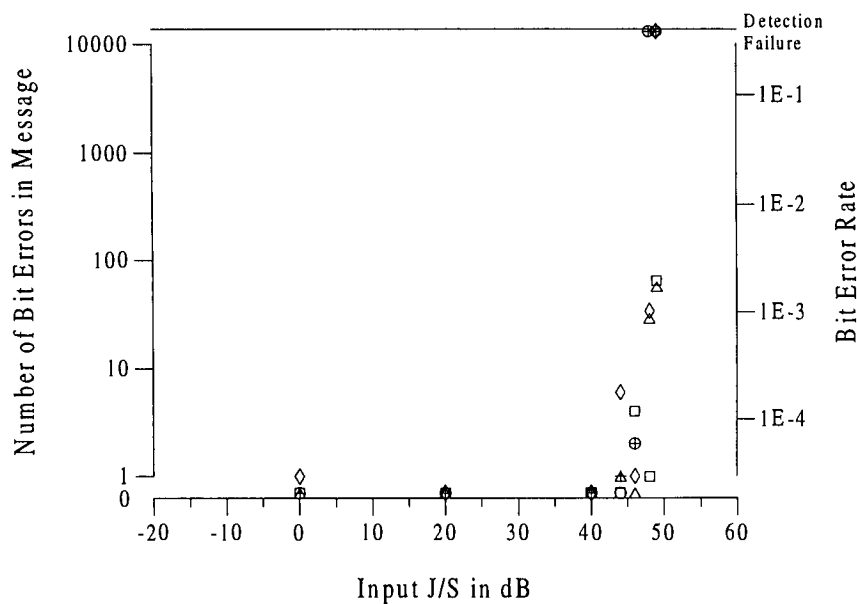
Chart 29: 4-PSK, continuous-noise jamming, 28.738 MHz, laboratory test, 45-degree jammer phase increments, uncoded.



4PJ4-18

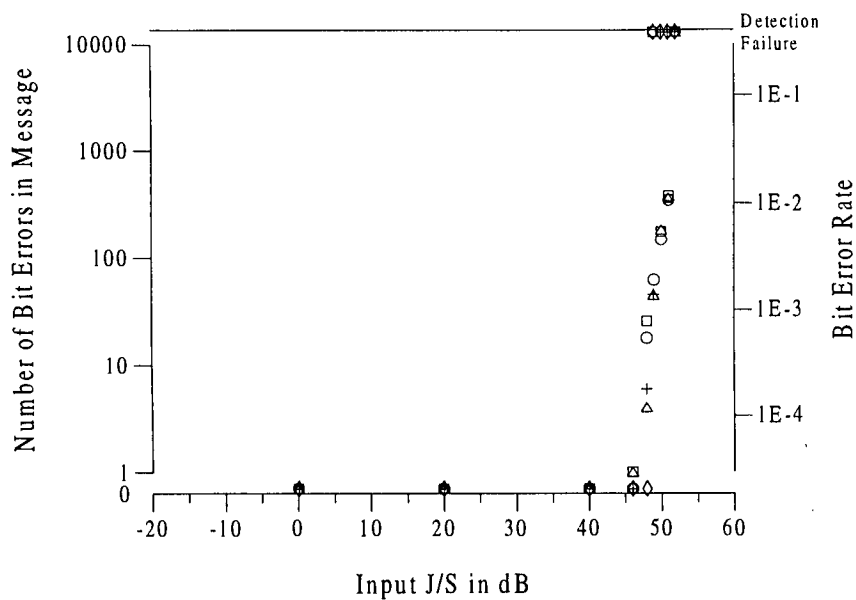
Chart 30: 4-PSK, continuous-noise jamming, 28.738 MHz, laboratory test, 90-degree jammer phase increments, uncoded.





4PJ4-21

Chart 31: 4-PSK, continuous-noise jamming, 28.738 MHz, laboratory test, 135-degree jammer phase increments, uncoded.



4PJ4-24

Chart 32: 4-PSK, continuous-noise jamming, 28.738 MHz, laboratory test, 180-degree jammer phase increments, uncoded.

SECURITY CLASSIFICATION OF FORM  
(highest classification of Title, Abstract, Keywords)

## DOCUMENT CONTROL DATA

(Security classification of title, body of abstract and indexing annotation must be entered when the overall document is classified)

<b>1. ORIGINATOR</b> (the name and address of the organization preparing the document. Organizations for whom the document was prepared, e.g. Establishment sponsoring a contractor's report, or tasking agency, are entered in Section 8)  Communications Research Centre 3701 Carling Avenue P.O. Box 11490, Station H Ottawa, Ontario Canada K2H 8S2		<b>2. SECURITY CLASSIFICATION</b> (overall security classification of the document including special terms if applicable)  UNCLASSIFIED
<b>3. TITLE</b> (the complete document title as indicated on the title page. Its classification should be indicated by the appropriate abbreviation (S,C,R or U) in parentheses after the title)  Field Trial Evaluation of the CRC Adaptive-Antenna Algorithm for the NATO STANAG 4285 Waveform (U)		
<b>4. AUTHORS</b> (Last name, first name, Middle initial)  Wu, K.H. and Tenne-Sens, A.		
<b>5. DATE OF PUBLICATION</b> (month and year of publication of document)  December 1997	<b>6a. NO. OF PAGES</b> (total containing information. Include Annexes, Appendices, etc.)  48	<b>6b. NO. OF REFS.</b> (total cited in document)  6
<b>7. DESCRIPTIVE NOTES</b> (the category of the document, e.g. technical report, technical note or memorandum. If appropriate, enter the type of report, e.g. interim, progress, summary, annual or final. Give the inclusive dates when a specific reporting period is covered.)  CRC Technical Report CRC-RP-97-004		
<b>8. SPONSORING ACTIVITY</b> (the name of the department project office or laboratory sponsoring the research and development. Include the address.)  Defence Research Establishment Ottawa(DREO) 3701 Carling Avenue Ottawa, Ontario CANADA K1A 0Z2		
<b>9a. PROJECT OR GRANT NO.</b> (if appropriate, the applicable research and development project or grant number under which the document was written. Please specify whether project or grant)  661-990-X21-998426156 - WK UNIT #1bb11	<b>9b. CONTRACT NO.</b> (if appropriate, the applicable number under which the document was written)  N/A	
<b>10a. ORIGINATOR'S DOCUMENT NUMBER</b> (the official document number by which the document is identified by the originating activity. This number must be unique to this document)  CRC Report No. CRC-RP-97-004	<b>10b. OTHER DOCUMENT NOS.</b> (Any other numbers which may be assigned to this document either by the originator or the sponsor)  N/A	
<b>11. DOCUMENT AVAILABILITY</b> (any limitations on further dissemination of the document, other than those imposed by security classification) <input checked="" type="checkbox"/> (X) Unlimited distribution <input type="checkbox"/> ( ) Distribution limited to defence departments and defence contractors; further distribution only as approved <input type="checkbox"/> ( ) Distribution limited to defence departments and Canadian defence contractors; further distribution only as approved <input type="checkbox"/> ( ) Distribution limited to government departments and agencies; further distribution only as approved <input type="checkbox"/> ( ) Distribution limited to defence departments; further distribution only as approved <input type="checkbox"/> ( ) Other (please specify)		
<b>12. DOCUMENT ANNOUNCEMENT</b> (any limitation to the bibliographic announcement of this document. This will normally correspond to the Document Availability (11). However, where further distribution (beyond the audience specified in 11) is possible, a wider announcement audience may be selected.)  UNLIMITED		

UNCLASSIFIED

SECURITY CLASSIFICATION OF FORM  
(highest classification of Title, Abstract, Keywords)

13. ABSTRACT (a brief and factual summary of the document. It may also appear elsewhere in the body of the document itself. It is highly desirable that the abstract of classified documents be unclassified. Each paragraph of the abstract shall begin with an indication of the security classification of the information in the paragraph (unless the document itself is unclassified) represented as (S), (C), (R), or (U). It is not necessary to include here abstracts in both official languages unless the text is bilingual).

(U) Results are presented for the evaluation of an adaptive-antenna algorithm designed for the NATO STANAG 4285 PSK (phase-shift keyed) waveform. The algorithm was developed at the Communications Research Centre and has been implemented on both the Andrew SciComm HF Adaptive-Antenna Receiving System (HFAARS or AN/FRQ-26) and the SED Systems Programmable HF Adaptive Receiving System (PHFARS); the tests reported here were conducted using the Andrew HFAARS. The goal was to evaluate the antijamming capability for groundwave or line-of-sight communications in the presence of various types of jamming signals. Performance of the system was characterized in terms of bit-error rate (BER) versus jamming-to-signal ratio (J/S) under various signal, jamming and propagation conditions. Under most of the test conditions reported, the algorithm was able to suppress the jamming signals by at least 40 dB.

10. KEYWORDS, DESCRIPTORS or IDENTIFIERS (technically meaningful terms or short phrases that characterize a document and could be helpful in cataloguing the document. They should be selected so that no security classification is required. Identifiers, such as equipment model designation, trade name, military project code name, geographic location may also be included. If possible keywords should be selected from a published thesaurus, e.g. Thesaurus of Scientific Terms (TEST) and that thesaurus-identified. If it is not possible to select indexing terms which are Unclassified, the classification of each should be indicated as with the title.)

Adaptive Antennas  
Algorithm Development  
AN/FRQ-26  
Antenna Arrays  
Antijamming  
Digital Signal Processing  
DSP  
HFAARS  
HF Communications  
Interference Cancellation  
Jamming Suppression  
PHFARS  
Pulsed Jamming  
NATO STANAG 4285  
Signal Detection  
TMS320C40

UNCLASSIFIED

SECURITY CLASSIFICATION OF FORM

INDUSTRY CANADA / INDUSTRIE CANADA



208893

